JOURNAL OF PETROLOGY | VOLUME 47 | NUMBER 8 | PAGES 1509–1530 | 2006 | doi:10.1093/petrology/egl017

Origin of the Pegmatitic Pyroxenite in the Merensky Unit, Bushveld Complex, South Africa

R. GRANT CAWTHORN* AND KEVIN BOERST

DEPARTMENT OF GEOSCIENCES, UNIVERSITY OF THE WITWATERSRAND, PO WITS, 2050, SOUTH AFRICA

RECEIVED MAY 20, 2005; ACCEPTED MARCH 3, 2006; ADVANCE ACCESS PUBLICATION MARCH 28, 2006

The genesis of the pegmatitic pyroxenite that often forms the base of the Merensky Unit in the Bushveld Complex is re-examined. Large (>1 cm) orthopyroxene grains contain tricuspidate inclusions of plagioclase, and chains and rings of chromite grains, which are interpreted to have grown by reaction between small, primary orthopyroxene grains and superheated liquid. This superheated liquid may have been an added magma or be due to a pressure reduction as a result of lateral expansion of the chamber. There would then have been a period of non-accumulation of grains, permitting prolonged interaction with the crystal mush at the crystal–liquid interface. Crystal ageing and grain enlargement of original orthopyroxene grains would ensue. Only after the pegmatitic pyroxenite had developed did another layer of chromite and pyroxenite, with normal grain size, accumulate above it. Immiscible sulphide liquids formed with the second pyroxenite, but percolated down as a result of their density contrast, even as far as the footwall anorthosite in some cases. Whole-rock abundances of incompatible trace elements in the pegmatitic pyroxenite are comparable with or lower than those of the overlying pyroxenite, and so there is no evidence for addition and/or trapping of large proportions of interstitial liquid, or of an incompatible-element enriched liquid or fluid in the production of the pegmatitic rock. Because of the coarse-grained nature of the rock, modal analysis, especially for minor minerals, is unreliable. Annealing has destroyed primary textures, such that petrographic studies should not be used in isolation to distinguish cumulus and intercumulus components. Geochemical data suggest that the Merensky pyroxenite (both pegmatitic and non-pegmatitic) typically consists of about 70–80% cumulus orthopyroxene and 10–20% cumulus plagioclase, with a further 10% of intercumulus minerals, and could be considered to be a heteradcumulate.

KEY WORDS: *Bushveld Complex; Merensky Reef; pegmatitic textures; cumulate processes; heteradcumulates; recrystallization; incompatible trace elements*

INTRODUCTION

The Bushveld Complex (Fig. 1a) is the world's largest layered intrusion (Wager & Brown, 1968; Willemse, 1969*a*; Eales & Cawthorn, 1996) and is famous for its platinum-group element (PGE), chromite and vanadiferous magnetite mineralization (Willemse, 1969*b*; Eales, 1987; Hatton & von Gruenewaldt, 1987; Barnes & Maier, 2002*a*; Cawthorn *et al.*, 2002*a*). The Merensky Reef is one of the most remarkable layers in any layered intrusion, carrying a near-constant grade of PGE (5–8 g/t) over a near-constant thickness (40–120 cm) over distances of over 100 km in both the western and eastern limbs (Wagner, 1929; Vermaak, 1976; Lee, 1996; Barnes & Maier, 2002*a*; Cawthorn *et al.*, 2002*a*). The mineralization occurs within a very distinctive sequence of layered rocks, but is not confined to a specific rock type. Typically (Fig. 2), there is a lower anorthosite or norite, overlain by a thin chromitite. In many sections there is an overlying feldspathic pyroxenite of variable grain size (up to 5 cm) and variable thickness (up to 40 cm). Additional chromitite layers may occur within and at the top of this pegmatitic pyroxenite. A feldspathic pyroxenite of normal grain size lies above the pegmatitic facies, and is up to 10 m thick. Overlying it is a thin norite followed by an upper anorthosite up to 12 m thick. The succession from the basal chromite to the top of the upper anorthosite is referred to as the Merensky Unit. In detail, many variations exist. For example, in some sections there is no pegmatitic pyroxenite and in others the PGE mineralization may occur in normal pyroxenite above the pegmatitic pyroxenite (Fig. 2).

There is a perceived view that the PGE mineralization is associated with the pegmatitic pyroxenite of the Merensky Unit, and many models have attempted to

*Corresponding author. Telephone +29 717 6557. Fax: +27 717 6579. E-mail: cawthorng@geosciences.wits.ac.za

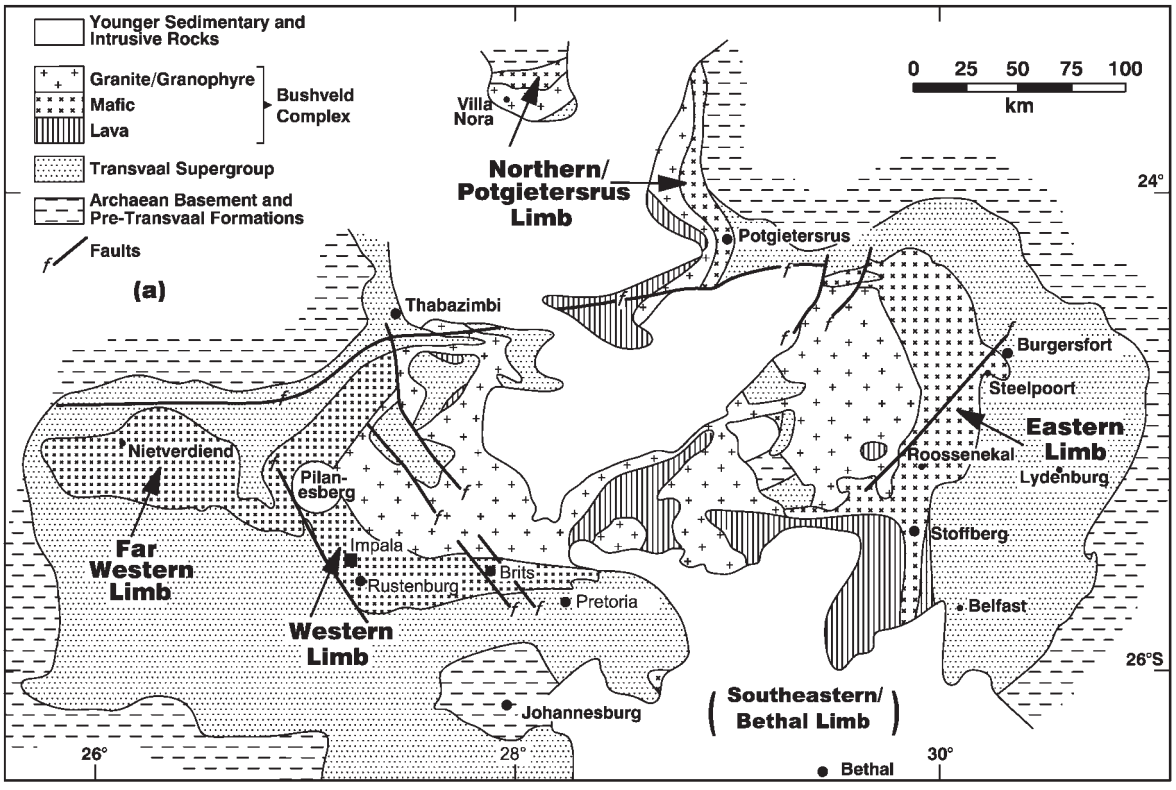

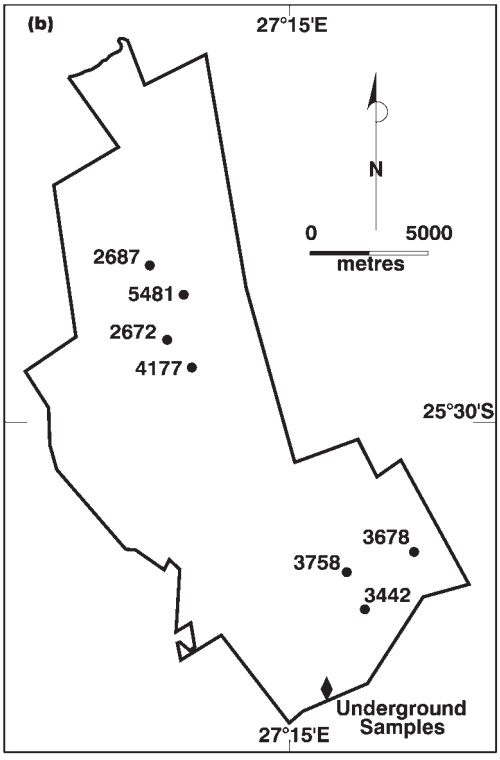

Fig. 1. (a) Simplified geological map of the Bushveld Complex. The location of Impala Platinum Mine is indicated. (b) Detail of the Impala Mine showing all borehole and underground sample localities for this study.

find a common process for the formation of the pegmatitic texture and the occurrence of the PGE mineralization. Many of these models appeal to the involvement of a late-stage, evolved, water-enriched magma, or a hydrothermal fluid, produced by fractionation of the magma (Lauder, 1970; Vermaak, 1976; von Gruenewaldt, 1979; Ballhaus & Stumpfl, 1985; Boudreau *et al.*, 1986; Mathez, 1989, 1995; Nicholson & Mathez, 1991; Boudreau, 1995; Mathez *et al.*, 1997). However, a number of high-temperature, primary magmatic processes have also been proposed (Naldrett *et al.*, 1986; Barnes & Campbell, 1988; Tredoux *et al.*, 1995; Viljoen, 1999; Viring & Cowell, 1999; Wilson *et al.*, 1999; Barnes & Maier, 2002*b*; Arndt *et al.*, 2005; Cawthorn, 2005; Cawthorn *et al.*, 2005). Both general models rely heavily upon the enlarged grain size of the pyroxene. Here, we emphasize that PGE mineralization is not confined to pegmatitic pyroxenite (Cawthorn *et al.*, 2002*a*). We re-examine the microscopic textures of these unusual pegmatitic pyroxenitic rocks and present geochemical data to test these various hypotheses.

For this study we obtained numerous continuous bore core intersections though the Merensky pyroxenite and its immediately underlying succession from the Impala Platinum Mine, west of Rustenburg (Fig. 1b). Previous studies on this mine have been reported by Leeb-du Toit (1986), Schurmann (1993), Cawthorn (1996) and Barnes & Maier (2002*b*).

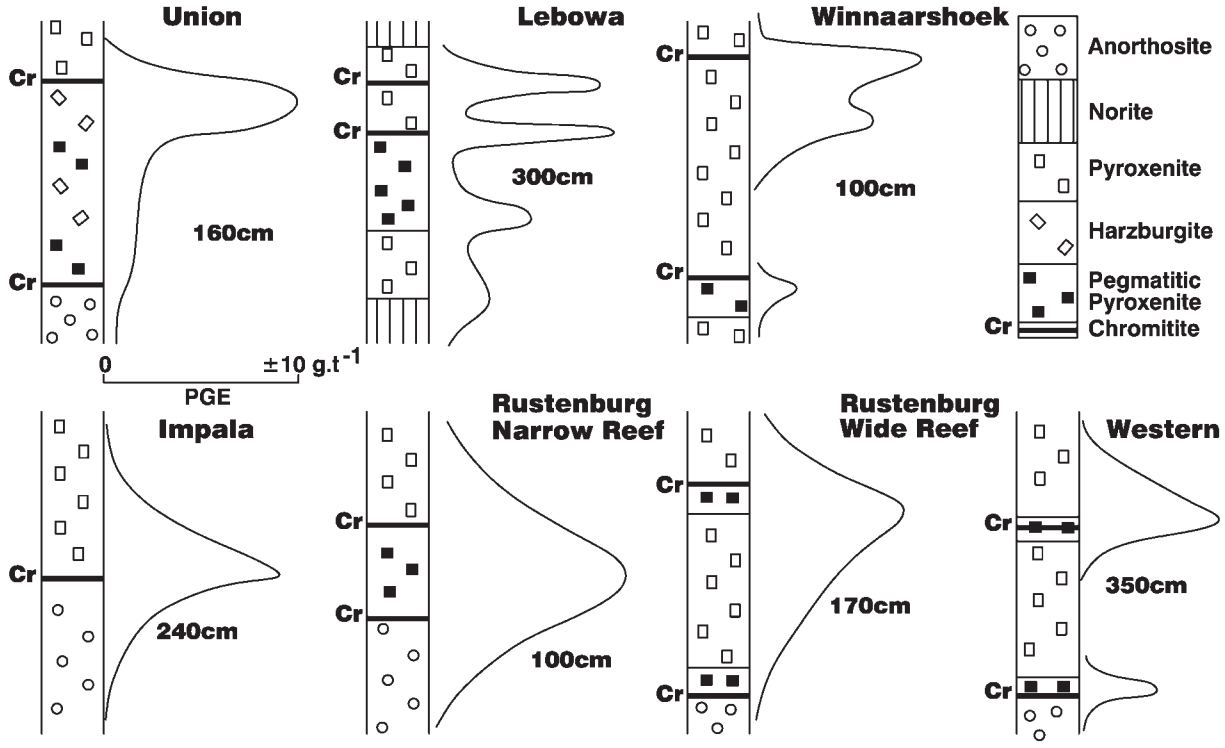

Fig. 2. Generalized sections of rock types and typical PGE distribution through the Merensky Reef in various mines. It should be noted that exact PGE concentrations through all mines are not always available from mining companies, and so the curves are sometimes semi-quantitative. Data sources have been given by Cawthorn *et al.* (2002*a*). The section for the Impala Mine refers to the northern half of the mine, where there is no pegmatitic pyroxenite. The typical section through the southern part of the mine is similar to that for the narrow reef, Rustenburg Mine.

A NOTE ON NOMENCLATURE

The name Merensky Reef has sometimes been rather loosely used in the scientific literature. Here, we restrict that term to the layers of rock, whatever their lithology, that contain potentially exploitable PGE mineralization. The Merensky Unit refers to the sequence from the basal chromitite, through various pyroxenites and norite to the top of the anorthosite. The Merensky pyroxenite occurs above the basal chromitite, may have a range of grain sizes, and may include further internal chromitite layers. The term normal pyroxenite refers to a rock with a grain size of less than 2 mm. Pegmatitic pyroxenite refers to rocks with a grain size of orthopyroxene greater than 2 mm (up to 5 cm). As described below, both pegmatitic and normal pyroxenite have mineral contents and textures that could be described by such terms as poikilitic and/or poikiloblastic, and can be variably feldspathic and sulphide-bearing; the terms pegmatitic pyroxenite and normal pyroxenite are used here for brevity and consistency. Many South African publications use the noun 'pegmatoid' to indicate a rock with a coarse texture, but lacking a granitic mineralogy. Here we use the adjective 'pegmatitic' in a purely textural sense with no implication about mineralogy or genesis.

FACIES CHANGES IN THE MERENSKY UNIT

Vertical sections through several facies of the Merensky Unit, in Fig. 2, show the locations of the PGE mineralization that defines the Merensky Reef in several of the mines around the Bushveld Complex. Some of the best-documented sections through the Merensky Unit come from the Rustenburg Platinum Mine (Fig. 2) (Vermaak, 1976; Kinloch, 1982; Ballhaus, 1988; Wilson *et al.*, 1999). At this mine the lower anorthosite is overlain by a thin chromitite layer followed by a pegmatitic pyroxenite, which changes abruptly into a normal grain size pyroxenite. There is usually another chromitite layer at the boundary between normal and pegmatitic pyroxenites. The normal pyroxenite shows a transition to norite, which is never very thick, followed by an upper anorthosite. This succession can be traced to the SE portion of the Impala Mine (Fig. 1a). However, the NW part of this mine shows only rare patches of pegmatitic pyroxenite, and the basal chromitite layer is overlain by normal pyroxenite (Fig. 2). The northwestward disappearance of the pegmatitic pyroxenite is irregular. PGE mineralization is equally well developed in both normal and pegmatitic pyroxenite, and is about 80 cm thick

(Leeb-du Toit, 1986). The only difference between the two reef types is that in the northern facies the mineralization straddles the basal chromite equally, whereas in the southern facies, there is less mineralization in the underlying anorthosite (Cawthorn *et al.*, 2002*b*). Various other facies of the Merensky Unit are known (Wagner, 1929; Viljoen, 1999; Cawthorn *et al.*, 2002*a*), but are not described or discussed in detail here. The relationship between the pegmatitic pyroxenitic facies and normal pyroxenitic facies in the Impala Mine is the main focus of this study.

PETROGRAPHY

Petrographic descriptions of the Merensky pyroxenite in the western limb have been presented by several researchers (e.g. Wagner, 1929; Vermaak, 1976; Lee, 1983; Wilson *et al.*, 1999; Barnes & Maier, 2002*b*). Their observations, and those from this study, can be summarized briefly. In the normal pyroxenite, orthopyroxene comprises about 80% of the rock as subhedral to polygonal grains typically 2 mm in size, with interstitial plagioclase. Clinopyroxene occurs as large (2 cm) grains that may have a euhedral outline, but contain variably abundant, partially resorbed orthopyroxene grains, giving rise to a pseudoporphyritic texture. Chromite is scarce, except within a few millimetres of the chromitite layers. In the pegmatitic pyroxenite, orthopyroxene grains range up to 5 cm in size, with shapes that can be euhedral to polygonal to subrounded. They form 60–90% of the rock. Olivine is often present as a minor phase, and may be euhedral or anhedral. Chromite grains occur sporadically within and on the grain boundaries of orthopyroxene. Clinopyroxene is rare, and occurs as small anhedral grains around the edges of orthopyroxene grains. Other interstitial to poikilitic minerals include mica, quartz, orthoclase and sulphides. There is almost no magmatic hornblende, although secondary amphibole, chlorite and sericite exist. It needs to be pointed out that it is not possible to determine quantitatively the proportions of minerals in this pegmatitic rock, especially for the minor minerals, because of the very coarse and irregular distribution of grains. Most previous comments on modal proportions are based on visual estimates and are quantitatively unreliable.

We recognize one distinctive petrographic aspect of some large pyroxene grains in the pegmatite that may provide constraints on its genesis. Some of the large grains of orthopyroxene contain inclusions, mainly of plagioclase, that have a very distinctive texture. The plagioclase grains have a tricuspidate shape with concave-inward boundaries (Fig. 3a) that are reminiscent of interstitial plagioclase grains in normal pyroxenite (Fig. 3e). Inspection of the shape of the orthopyroxene grain surrounding plagioclase in Fig. 3a gives the impression that there were a number of originally euhedral orthopyroxene grains with interstitial plagioclase, but which now have developed a common optical orientation, and thus appear as a single grain. Occasionally, the enclosed plagioclase grains are associated with numerous small chromite grains (Fig. 3b) that define elongate clusters, or even a tricuspidate shape. Complete rings of chromite grains also occur embedded inside a large orthopyroxene grain (Fig. 3c), and possibly define the shape and size of an original orthopyroxene grain. However, optical continuity of the orthopyroxene extends far beyond the limits of this chromite circle. For comparison, Fig. 3e illustrates the texture frequently observed in chromitic feldpathic pyroxenite of normal grain size. This texture is generally interpreted as being due to the co-accumulation of orthopyroxene and small chromite grains, cemented by plagioclase.

Exactly the same negative shape plagioclase grains in large orthopyroxene grains occur in the pegmatite below the Upper Group 2 chromitite layer (Cawthorn & Barry, 1992) and in other stratabound pegmatitic layers.

We also note that large grains of olivine can also contain inclusions, in some cases polyphase, of orthopyroxene, plagioclase and clinopyroxene (Fig. 3d). However, these included minerals do not preserve an interstitial texture, and so their genesis is less definitive than the textures in Fig. 3a–c.

One petrographic feature needs to be mentioned here to reinforce some of the arguments presented below. Wagner (1929) described a texture, duplicated here as Fig. 4, from the pegmatitic pyroxenite in the Merensky Unit in the eastern limb. A very thin layer of chromite grains runs through the middle of a number of atypically large orthopyroxene grains. Its significance is discussed below.

GEOCHEMISTRY

Many analyses of the Merensky pyroxenite have been published. Most are of isolated samples, and so it cannot be confirmed that such analyses are totally representative of the entire layer. This problem is specifically relevant when dealing with the pegmatitic pyroxenite where large variations in grain size and mineral proportions occur over short distances. The only studies in which borehole core has been analysed from continuous sections are by Lee (1983) and Wilson *et al.* (1999) from the Rustenburg Mine and by Barnes & Maier (2002*b*) from the Impala Mine. All these profiles included a basal pegmatitic pyroxenite of variable thickness.

For our study we have analysed continuous core from six boreholes or channel-cut samples from underground workings containing pegmatitic pyroxenite and eight

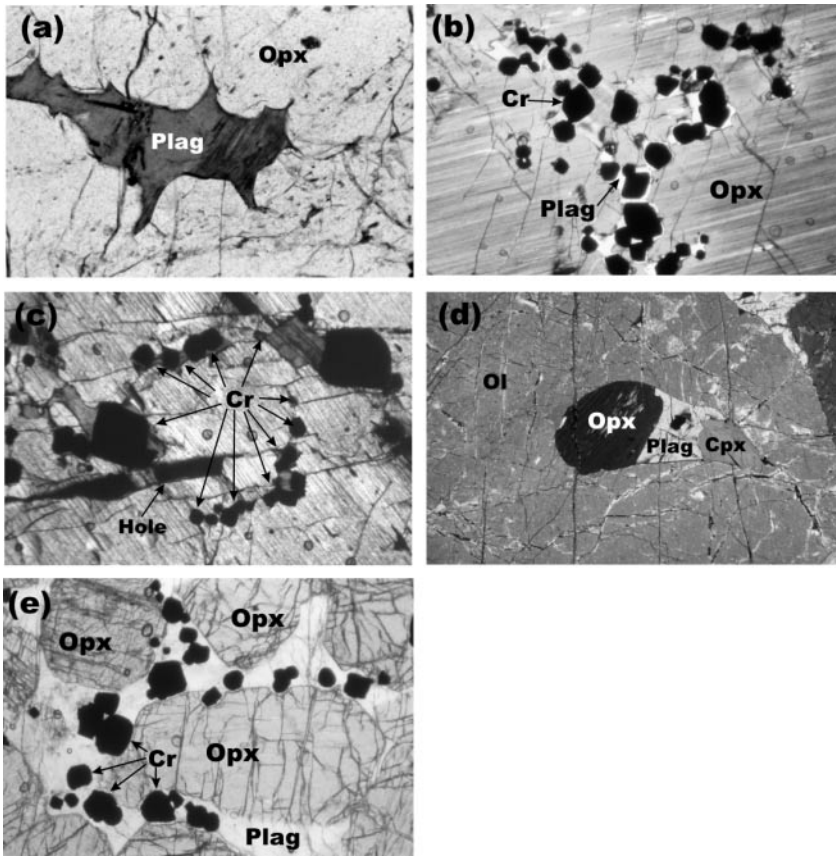

Fig. 3. Photomicrographs of various pyroxenitic rocks: (a)–(d) are of the pegmatitic pyroxenite, and (e) is of normal pyroxenite. (a) A large, optically continuous, grain of orthopyroxene containing a plagioclase grain (dark grey) with numerous cusps and concave boundaries. (b) A single grain of orthopyroxene showing multiple twin lamellae with inclusions of discrete chromite grains embedded in plagioclase, in a tricuspidate arrangement. (c) Ring of chromite grains in the middle of an optically continuous orthopyroxene grain. (d) Large olivine grain with a polyphase inclusion of orthopyroxene (dark on left), plagioclase (pale in centre) and clinopyroxene (similar grey to olivine but with cleavage and no fractures on right). (e) Euhedral orthopyroxene grains with cumulus chromite grains concentrated around the edges, set in a single interstitial plagioclase grain with highly irregular concave margins against the orthopyroxene. Ol, Opx, Cpx, Plag and Cr refer to olivine, orthopyroxene, clinopyroxene, plagioclase and chromite, respectively. Width of all photomicrographs is 4 mm.

where only normal pyroxenite occurs (Fig. 1b). It is emphasized that no intersection near a pothole (circular structures where the underlying stratigraphic succession has been excavated to varying depths) was used. Samples were usually taken from 1 m into the underlying rocks to 1 m above the basal chromitite contact. Some underground channel samples extended a shorter interval up and down, because of the limited mining width.

Core of pegmatitic pyroxenite was cut into 10 cm lengths. Other rock types were cut into 20 cm sample lengths to minimize the number of samples per profile that had to be analysed. Core diameter is 3·6 cm. The size of samples cut from channels was more variable, but their mass was comparable with that of the core samples. Any layers of chromite or irregular patches enriched in chromite were cut from the samples prior to further processing because complete fusion for X-ray fluorescence (XRF) analysis of chromite-rich samples was not possible. After a thin slice was removed for thin-section study, half the sample was crushed for whole-rock chemical analysis and the other half was used to prepare mineral concentrates by coarse crushing to 0·1 mm, and separation using a Franz magnetic separator. All analyses were performed using a Phillips PW1400 XRF spectrometer at the University of the Witwatersrand. Whole-rock and mineral-concentrate analyses for orthopyroxene and plagioclase for two sections, one with and one without pegmatitic pyroxenite, are given in Tables 1, 3 and 4. However, these two profiles include only two analyses from the pegmatitic pyroxenite and 18 from the normal pyroxenite, and so we have added further analyses in Table 2 of the pegmatitic pyroxenite and its mineral concentrates from four other profiles for comparison. Complete databases were presented by Boerst (2001).

Geochemical logs of important whole-rock parameters (Table 1) are included in Fig. 5. Most of the major and

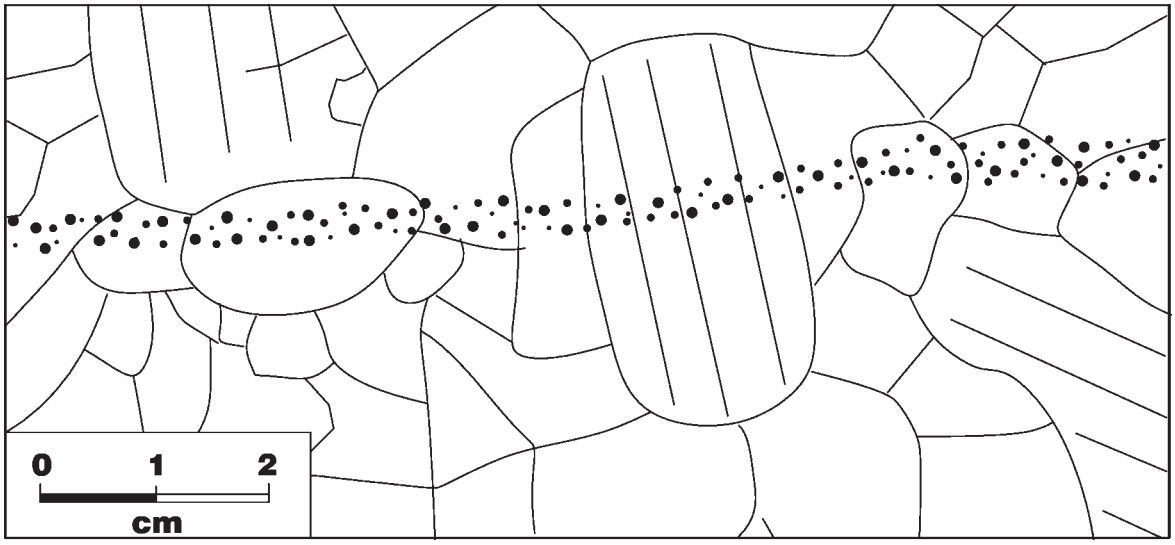

Fig. 4. Reproduction of a diagram from Wagner (1929) showing a thin layer of chromite grains running through the middle of a number of large orthopyroxene grains.

minor oxides reflect the proportion of the major minerals in the rock. For example, SiO_2 contents in plagioclase and orthopyroxene are about 49 and 53%, and so the two major rock types, anorthosite and pyroxenite, have values within this range. Similar arguments apply to the whole-rock abundances of MgO and FeO (in pyroxene) and Al_2O_3 and CaO (in plagioclase). Up to 10% olivine and chromite may be present in the pegmatitic pyroxenite. MgO is 1–2% higher and SiO_2 up to 5% lower (Table 2) in the pegmatitic pyroxenite than in the normal pyroxenite, indicating these mineralogical differences. Cr contents in the normal pyroxenite are typically 2500–3200 ppm, held largely in the orthopyroxene that contains 3200–3600 ppm Cr (Table 3). The highest Cr contents in the pegmatitic pyroxenite reach over 30 000 ppm (and are probably not accurate, as XRF standards cover the range only up to 5000 ppm), equivalent to 10% by weight chromite in the rock. TiO_2 is a minor component of orthopyroxene (0·3%) and is absent in plagioclase, and so whole-rock TiO_2 contents are typically 0·1 and 0·3% in the anorthosite and pyroxenite, respectively.

The abundance of Cu reflects the presence of sulphide phases and so locates the zones of greatest mineralization (located where Cu values exceed 1000 ppm). In the Merensky Reef, Cu and PGE abundances are closely correlated, as shown by Lee (1996) and Barnes & Maier (2002*b*). It should be noted that in both profiles in Fig. 5, Cu values are significant in the anorthosite below the basal chromitite, and not only in the pyroxenite. Ni is present in both sulphide and orthopyroxene and so displays three abundance levels, <300 ppm in unmineralized anorthosite, 500–700 ppm in unmineralized pyroxenite, and >1000 ppm in mineralized samples of both rock types. Thus, the individual oxide and Cu and Ni abundances provide little genetic information that cannot be determined from the petrography.

The abundances in the whole rocks of those trace elements that are incompatible in plagioclase and orthopyroxene reflect the proportion of trapped magma that finally crystallized the interstitial phases in the rock. Of these elements, the abundance of P_2O_5 and Y are below or close to detection limits (0·02% and 5 ppm, respectively) and are excluded from all tables. Zr and K can be used to reflect the proportion of trapped liquid, although K is also present in plagioclase in the range from below detection limit to 0·3% K_2O (Table 4), and Zr in orthopyroxene is 5–20 ppm (Table 3). These abundances are not trivial when compared with the whole-rock content, and so these elements are not perfect indicators of trapped liquid content. In principle, if the concentration observed in these major minerals, multiplied by the cumulus modal proportion of the mineral, is subtracted from the whole-rock abundances, the remainder reflects this interstitial component (see below). K_2O values are typically <0·1% in all rock types. In sections through both pyroxenites in Fig. 5, there is an upward increase to 0·3%, followed by a decrease to 0·1% in the pegmatitic pyroxenite, the maximum occurring ~40 cm above the base of the pyroxenite. Zr contents show parallel trends in both pyroxenite types, again with higher values more than 40 cm above the base.

Mineral compositions are given in Tables 3 and 4 and shown in Figs 6 and 7. A measure of the purity of the mineral concentrates can be obtained by inspection of the Cr content of plagioclase and Sr content of

Table 1: Whole-rock analyses from two vertical sections, one with and one without a pegmatitic pyroxenite

Height in cm	SiO_2	TiO_2	Al_2O_3	Fe_2O_3 (T)	MnO	MgO	CaO	Na_2O	K_2O	Rb	Sr	Zr	Ni	Cu	Cr
Section through normal pyroxenite with no pegmatitic pyroxenite (bore core 5481)															
+90–100	51·76	0·25	5·87	11·59	0·32	23·45	4·05	0·67	0·28	17	71	26	1031	260	2518
+80–90	51·68	0·22	6·31	11·65	0·10	23·57	4·52	0·84	0·11	14	83	31	902	200	2578
+70–80	53·73	0·25	5·68	11·88	0·07	23·58	4·03	0·80	0·20	15	79	31	859	141	2918
+60–70	52·96	0·21	6·56	11·45	0·14	23·35	4·39	0·78	0·11	19	70	47	860	161	2786
+50–60	52·06	0·25	5·59	11·73	0·10	24·01	4·16	0·76	0·19	19	71	51	816	153	2526
+40–50	52·70	0·29	6·17	11·48	0·10	23·31	4·41	0·83	0·32	20	79	49	778	132	2579
+30–40	52·63	0·25	5·53	12·20	0·10	23·74	4·08	0·79	0·14	15	79	24	823	112	2656
+20–30	52·93	0·24	6·16	11·40	0·16	23·81	4·64	0·77	0·09	14	75	23	791	72	2923
+10–20	52·10	0·25	5·56	12·42	0·21	23·76	4·58	0·71	b.d.	12	73	23	1875	860	2740
0–10	49·70	0·30	4·56	14·62	0·20	24·49	3·91	0·59	b.d.	11	56	24	5289	2722	2866
−20–0	48·47	0·10	26·49	3·46	0·10	4·48	19·94	2·00	0·08	11	414	11	1504	683	419
−40–20	48·85	0·11	24·64	4·31	0·05	6·39	12·94	1·88	b.d.	10	380	12	1350	644	611
−60–40	48·76	0·11	23·96	3·94	0·20	7·26	12·81	1·83	b.d.	10	368	13	366	68	792
−80–60	49·02	0·11	23·60	3·84	0·50	7·13	12·69	1·90	b.d.	9	377	12	259	15	753
−100–80	48·82	0·11	23·56	3·72	0·64	7·36	12·57	1·90	b.d.	10	378	11	254	9	787
Section with pegmatitic pyroxenite from 0 to 20 cm above basal chromitite (bore core 3442)															
+90–100	51·92	0·26	5·14	12·30	0·12	23·61	4·99	0·67	0·10	14	60	26	2209	1052	3099
+80–90	53·14	0·27	5·33	12·32	0·04	23·52	4·80	0·73	0·13	16	61	60	1699	677	3155
+70–80	53·53	0·25	5·80	11·64	0·09	23·60	4·34	0·77	0·15	70	67	23	1167	347	3055
+60–70	52·90	0·29	4·86	11·74	0·18	23·85	4·15	0·69	0·25	22	52	81	998	247	2573
+50–60	53·12	0·27	5·56	11·78	0·10	23·46	3·53	0·74	0·19	20	62	42	934	199	2778
+40–50	52·51	0·26	5·25	11·83	0·08	23·82	3·79	0·68	0·20	18	61	36	997	231	2606
+30–40	51·92	0·26	5·33	12·61	0·13	23·80	3·91	0·51	0·12	13	55	32	1780	797	2517
+20–30	48·69	0·29	5·22	15·28	0·10	23·15	4·31	0·40	b.d.	8	54	16	6855	3294	5720
+10–20	43·23	0·43	4·83	17·80	b.d.	24·94	2·32	0·09	b.d.	13	47	28	7814	3345	26547
0–10	42·80	0·19	6·29	13·33	0·05	26·66	3·11	0·25	b.d.	10	69	15	3290	979	11571
−20–0	47·62	0·11	23·14	6·20	0·10	8·57	11·96	1·74	0·07	8	346	10	3339	1968	1095
−40–20	48·77	0·11	23·63	5·06	0·10	7·34	12·34	1·94	b.d.	9	365	10	2433	1332	825
−60–40	48·80	0·10	23·48	5·08	0·15	7·50	12·13	1·94	0·09	9	357	10	2501	1036	896
−80–60	49·77	0·11	23·32	4·23	0·05	8·43	12·10	1·89	0·04	10	352	13	1221	413	998
−100–80	49·75	0·11	23·06	4·72	0·10	8·34	11·89	2·21	0·04	10	355	7	305	17	986

Height in cm is measured relative to the basal chromitite. Bore core locations are shown in Fig. 1b. Oxide content is given in weight %, trace element content in ppm. Analyses were performed on a Phillips PW1400 XRF spectrometer in the School of Geosciences, University of the Witwatersrand. b.d., below detection limits; n.a., not analysed.

orthopyroxene, each element being abundant in the other mineral (orthopyroxene and plagioclase, respectively) that is the most likely impurity in the mineral concentrates. Sr in the orthopyroxene concentrates ranges from 2 to 16 ppm and Cr in plagioclase ranges from 9 to 77 ppm. Plagioclase contains about 400 ppm Sr. Hence the orthopyroxene concentrates contain from 0·5 to 4% impurity. Some of the higher values occur in the pegmatitic pyroxenite, probably because of the inclusions of plagioclase described above. Orthopyroxene contains ±3500 ppm Cr. If the plagioclase concentrates contained orthopyroxene, the Cr values would indicate 0–2% impurity. However, it is equally possible that there are chromite inclusions in the plagioclase, in which case a maximum of only 0·025% impurity would be required.

For orthopyroxene (Fig. 6) the mg value [100 × Mg/(Mg + Total Fe)] is in the range 77–82 for anorthosite, 80–81 for normal pyroxenite, and 81–84 for pegmatitic pyroxenite. The mg value for orthopyroxene from the pegmatitic pyroxenite is slightly greater than in the normal pyroxenite, and this difference is considered real. Zoning is not observed in orthopyroxene in electron microprobe studies (Eales *et al.*, 1993).

Table 2: Whole-rock and mineral-separate analyses of pegmatitic pyroxenite from four other vertical sections

Borehole no. and height in cm	SiO_2	TiO_2	Al_2O_3	Fe_2O_3 (T)	MnO	MgO	CaO	Na_2O	K_2O	Rb	Sr	Zr	Ni	Cu	Cr
Whole-rock analyses															
3678 (10–20)	44·05	0·48	7·45	15·80	0·19	21·00	4·68	0·59	b.d.	11	77	17	4729	2463	32247
3758 (10–20)	43·90	0·58	7·52	17·14	0·51	20·69	5·18	0·59	b.d.	8	65	17	6042	2855	32086
3758 (0–10)	46·23	0·16	11·58	10·23	0·11	21·28	6·09	0·71	b.d.	9	141	14	1748	509	14865
PP1 (50–60)	45·14	0·73	8·65	16·20	0·11	20·20	4·46	0·86	b.d.	11	103	21	3652	2143	32656
PP1 (40–50)	50·07	0·22	8·96	11·49	b.d.	21·27	5·44	0·90	b.d.	11	130	23	2031	1010	8247
PP1 (30–40)	50·69	0·20	9·91	9·99	b.d.	20·25	6·21	1·09	b.d.	11	144	21	1633	780	2766
PP1 (20–30)	52·37	0·33	4·26	15·36	b.d.	23·00	4·22	0·40	0·19	20	38	36	4619	3729	2623
PP1 (10–20)	51·06	0·28	4·99	13·38	b.d.	23·46	5·16	0·55	b.d.	13	60	28	3184	2114	2640
PP1 (0–10)	47·48	0·20	5·93	16·41	b.d.	23·05	4·50	0·50	b.d.	9	78	19	6221	2730	2028
PP2 (30–40)	48·04	0·68	3·07	14·97	0·20	22·32	9·12	0·25	b.d.	10	16	30	5788	1675	17595
PP2 (20–30)	51·23	0·20	8·07	11·96	0·07	23·31	4·57	0·83	b.d.	11	99	16	2633	1524	8886
PP2 (10–20)	49·10	0·28	11·54	10·80	0·03	20·08	5·76	1·12	0·05	14	150	20	926	260	17630
PP2 (0–10)	44·00	0·22	8·90	13·60	0·06	22·74	5·29	0·45	b.d.	10	135	31	3693	1405	5758
PP3 (20–10)	44·11	0·20	8·88	13·17	0·17	23·31	5·09	0·38	b.d.	12	150	19	4796	1739	8993
PP3 (0–10)	50·18	0·23	7·64	12·10	0·15	22·63	5·30	0·60	0·06	12	104	17	3488	1785	5594
Orthopyroxene compositions															
3678 (10–20)	54·13	0·25	1·77	12·39	0·22	29·78	1·75	n.a.	b.d.	b.d.	4	7	768	b.d.	3403
3758 (10–20)	54·20	0·29	1·35	13·68	0·22	29·85	1·50	n.a.	b.d.	b.d.	b.d.	7	1002	46	3540
3758 (0–10)	53·80	0·24	1·57	12·29	0·23	30·19	1·67	n.a.	b.d.	b.d.	b.d.	10	824	21	3769
PP1 (40–60)	52·00	0·27	2·10	13·23	0·23	28·90	2·09	n.a.	b.d.	b.d.	14	22	1151	284	7320
PP1 (20–40)	52·16	0·22	1·58	14·50	0·23	29·55	1·92	n.a.	b.d.	b.d.	6	19	1278	307	3630
PP1 (0–20)	51·42	0·22	1·77	14·27	0·25	28·75	2·37	n.a.	b.d.	b.d.	15	21	1659	535	3562
Plagioclase compositions															
3678 (10–20)	49·65	0·12	31·40	0·38	0·06	0·34	14·09	3·12	0·08	b.d.	460	n.a.	30	79	76
3758 (10–20)	51·14	0·14	30·57	0·38	0·06	0·52	13·81	3·45	0·09	b.d.	458	n.a.	108	176	26
3758 (0–10)	49·37	0·13	31·97	0·41	0·07	0·51	15·16	2·54	b.d.	b.d.	458	n.a.	65	131	49
PP1 (40–60)	50·76	0·05	30·67	0·70	0·04	0·32	14·14	3·24	0·12	b.d.	469	n.a.	278	102	160
PP1 (20–40)	50·63	0·11	30·06	1·32	b.d.	0·31	13·89	3·20	0·12	b.d.	457	n.a.	716	60	21
PP1 (0–20)	50·38	0·05	30·35	1·00	b.d.	0·43	14·29	3·14	0·23	b.d.	473	n.a.	848	67	20

See legend to Table 1. PP1, PP2 and PP3 refer to sections taken underground (see Fig. 1b).

Analysis for Cr by XRF of mineral concentrates has advantages and disadvantages compared with electron microprobe techniques. Cr could be present as inclusions of chromite in the orthopyroxene mineral concentrates, increasing apparent Cr abundance in analyses of mineral concentrates. Because chromite contains 300 000 ppm Cr, the presence of 0·1% of inclusions would increase the apparent Cr content by 300 ppm. However, for electron microprobe values that have been reported in detail, the range of values quoted for multiple analyses of a single sample is large. For example, Schurmann (1993) gave averages for Cr_2O_3 typically of 0·4%, but with a total range that exceeds 0·1% (i.e. 25% of the total concentration). Specifically, for a single section of Merensky pyroxenite, he quoted a range from 0·35 to 0·5% Cr_2O_3 for seven analyses. We suggest that the greater precision obtainable by XRF spectrometry outweighs the potential problems of inclusions in mineral concentrates. Concentrations reported here (Tables 2 and 3) are in the range 3200 and 3600 ppm, and are relatively constant regardless of rock type. Such contents are comparable with the averages in pyroxene obtained by electron microprobe at this level of the intrusion given by Schurmann (1993) and Eales *et al.* (1993).

Plagioclase ought to preserve zoning because of the extremely slow, coupled diffusion between NaSi and CaAl (Morse, 1984). However, in this study the compositions are the averages of the entire mineral, incorporating the more albitic rims (Fig. 7). The plagioclase concentrates in the anorthosites have near-constant An content (77–79). In the lowest 20 cm of both types of pyroxenite

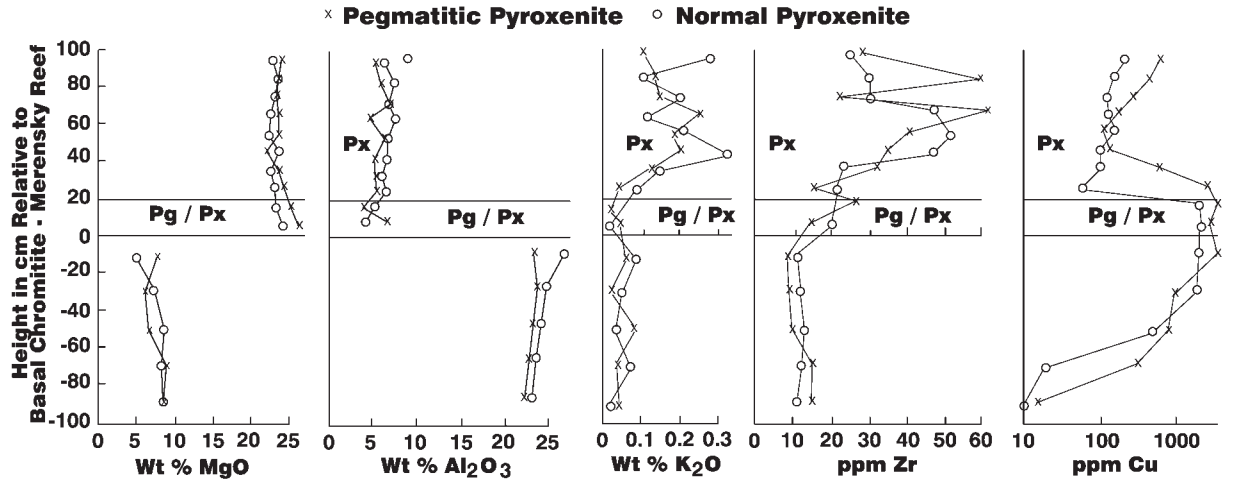

Fig. 5. Whole-rock geochemical variation through the underlying rocks and the Merensky pyroxenite. Data are shown from two profiles: one through a section where there is a 20 cm thick pegmatitic pyroxenite layer, and one where the entire pyroxenite layer is of normal grain size. Datum is the base of the pyroxenite at which there is a thin chromitite layer. The interval 0–20 cm is designated Pg/Px to indicate that the samples may be of pegmatitic or normal grain size. ×, Samples from the profile with a pegmatitic layer; ○, samples from the profile with no pegmatitic pyroxenite. Four other profiles through pegmatitic pyroxenite facies, and six profiles where there is no pegmatitic pyroxenite, all gave the same trends (Boerst, 2001).

Table 3: Orthopyroxene compositions determined on mineral separates from selected samples in Table 1

Height In cm	SiO_2	TiO_2	Al_2O_3	Fe_2O_3 (T)	MnO	MgO	CaO	Sr	Zr	Ni	Cu	Cr
Section through normal pyroxenite with no pegmatitic pyroxenite (bore core 5481)												
+90–100	54·33	0·27	1·24	13·99	0·24	29·49	1·30	b.d.	7	764	b.d.	3022
+70–80	51·90	0·20	1·54	13·49	0·24	29·47	1·99	5	19	721	45	3343
+60–70	53·48	0·22	1·47	13·94	0·24	29·78	1·67	5	19	689	37	3301
+50–60	53·95	0·22	1·42	13·98	0·25	29·26	1·73	6	18	691	30	3312
+40–50	53·79	0·24	1·42	13·82	0·25	29·17	1·76	5	19	678	40	3297
+30–40	52·45	0·22	1·34	13·54	0·24	29·94	1·71	7	21	706	50	3326
+20–30	53·05	0·22	1·81	13·65	0·24	29·83	2·02	10	19	702	31	3357
+10–20	53·58	0·23	2·01	14·11	0·22	28·49	1·89	8	19	937	175	3397
0–10	54·12	0·29	1·20	13·84	0·25	29·73	1·27	b.d.	9	973	8	3434
−20–0	53·76	0·27	1·29	15·08	0·24	28·75	1·11	b.d.	10	984	b.d.	2435
−100–80	54·44	0·27	1·44	13·52	0·24	29·54	1·36	5	7	595	b.d.	3326
Section with pegmatitic pyroxenite from 0 to 20 cm above basal chromitite (bore core 3442)												
+90–100	54·28	0·27	1·43	13·28	0·23	29·55	1·57	b.d.	6	843	b.d.	3490
+70–80	53·17	0·22	1·63	13·53	0·26	29·90	1·82	5	19	807	64	3443
+60–70	53·42	0·22	2·34	13·49	0·25	28·78	2·11	b.d.	21	758	33	3402
+50–60	53·26	0·23	1·56	13·79	0·23	29·69	1·77	5	19	748	28	3337
+40–50	53·75	0·23	1·73	13·58	0·24	29·13	1·77	b.d.	20	751	20	3325
+20–30	53·51	0·27	1·94	13·23	0·25	29·42	1·60	b.d.	5	1240	219	3742
+10–20	54·54	0·26	1·87	11·13	0·23	30·30	1·76	14	17	822	65	3270
0–10	53·79	0·22	2·49	11·06	0·22	29·71	2·18	16	9	675	b.d.	3526
−20–0	53·52	0·25	1·91	13·14	0·23	29·83	1·50	7	6	1030	b.d.	3430
−100–80	53·47	0·27	1·87	12·71	0·22	30·19	1·57	5	9	634	b.d.	3632

See legend to Table 1.

Table 4: Plagioclase compositions determined on mineral separates from selected samples in Table 1

Height in cm	SiO_2	TiO_2	Al_2O_3	Fe_2O_3 (T)	MgO	CaO	Na_2O	K_2O	Sr	Ni	Cu	Cr
Section through normal pyroxenite with no pegmatitic pyroxenite (bore core 5481)												
+90–100	53·40	0·14	28·96	0·48	0·50	12·66	3·80	0·01	439	24	65	27
+70–80	53·27	0·04	28·52	1·18	0·66	12·77	3·55	0·06	435	31	9	62
+60–70	54·23	0·05	28·03	0·74	0·85	12·20	3·59	0·10	414	45	12	65
+50–60	53·79	0·04	28·49	0·64	0·70	12·40	3·66	0·21	421	32	13	60
+40–50	53·33	0·09	28·47	0·63	0·52	12·29	3·48	0·32	418	28	13	72
+30–40	52·12	0·11	29·90	0·66	0·66	12·95	3·51	0·24	425	38	20	68
+20–30	51·62	0·04	30·20	0·58	0·64	13·57	3·43	0·18	434	25	10	73
+10–20	50·47	0·04	29·42	0·84	0·71	13·75	3·40	0·13	435	180	140	77
0–10	51·57	0·11	28·87	1·81	0·46	13·03	3·42	0·11	422	609	157	37
−20–0	48·60	0·11	32·61	0·36	0·35	15·89	2·30	0·00	459	37	32	9
−100–80	48·93	0·10	32·35	0·34	0·48	15·58	2·27	0·00	462	15	2	24
Section with pegmatitic pyroxenite from 0 to 20 cm above basal chromitite (bore core 3442)												
+90–100	52·78	0·12	29·57	0·50	0·73	13·08	3·19	0·04	434	36	242	22
+70–80	52·77	0·06	29·25	0·69	0·61	12·90	3·45	0·09	427	45	146	45
+60–70	53·94	0·14	28·19	0·77	0·81	12·27	3·40	0·09	403	38	130	55
+50–60	54·90	0·05	27·67	0·82	0·91	12·02	3·35	0·06	402	51	150	51
+40–50	52·68	0·06	27·87	0·78	0·84	13·32	3·25	0·08	408	41	98	55
+20–30	49·86	0·17	30·18	1·00	0·93	13·74	3·01	0·03	446	864	396	32
+10–20	47·87	0·03	30·35	2·10	0·83	15·94	2·12	0·01	460	30	79	76
0–10	49·86	0·04	30·84	1·51	1·59	14·05	2·82	0·12	473	75	169	9
−20–0	48·33	0·08	31·77	0·48	0·45	14·84	2·44	0·00	462	95	199	26
−100–80	49·33	0·11	31·23	0·42	0·78	15·18	2·27	0·02	447	29	12	58

See legend to Table 1.

values range from 65 to 80, with the higher values comparable with those in the underlying anorthosite. In contrast, in the overlying 80 cm of pyroxenite, the values are typically less than 70. K_2O contents are typically less than 0·1%, except at about 40 cm height above the pegmatitic pyroxenite.

FORMATION OF PEGMATITIC TEXTURES

We suggest that the textures shown in Fig. 3 provide crucial constraints on the genesis of these rocks and so we begin our discussion with our interpretation of these textures. It is suggested that the large grains of orthopyroxene in Fig. 3c formed by annealing of many small, euhedral, primary grains, such as those seen in the typical feldspathic pyroxenite of Fig. 3e. The outline of the original shapes of small grains can still be identified when in proximity to plagioclase or chromite. The texture seen in the coarse-grained rock (Fig. 3a) suggests that the shape of the original interstitial plagioclase has been preserved. These plagioclase grains have inward cuspate boundaries and are fundamentally different in their shape and genesis from the rounded plagioclase grains described by Eales *et al.* (1991), from a number of pyroxenite layers of the Upper Critical Zone. Eales *et al.* (1991) suggested that the rounded grains had survived in suspension in an added, hotter magma and had partially redissolved to produce a rounded shape before being engulfed in growing orthopyroxene grains. Such a process could not produce the shapes of grains we describe here.

We now turn to the textural feature shown in Fig. 4. Wagner (1929) suggested that 'chromite grains... remained suspended in the magma at a certain level and that the silicates crystallized round them'. This process would require that all those orthopyroxene grains subsequently sank as a single continuous sheet, so that perfect continuity of the chromite inclusions was not broken. Given the size and density of the orthopyroxene grains, we consider such a process unlikely. We suggest that it is more likely that two discrete layers of normal grain size pyroxenite formed with an intervening thin chromite layer. The above proposed reconstitution process occurred that coarsened the grain size of the

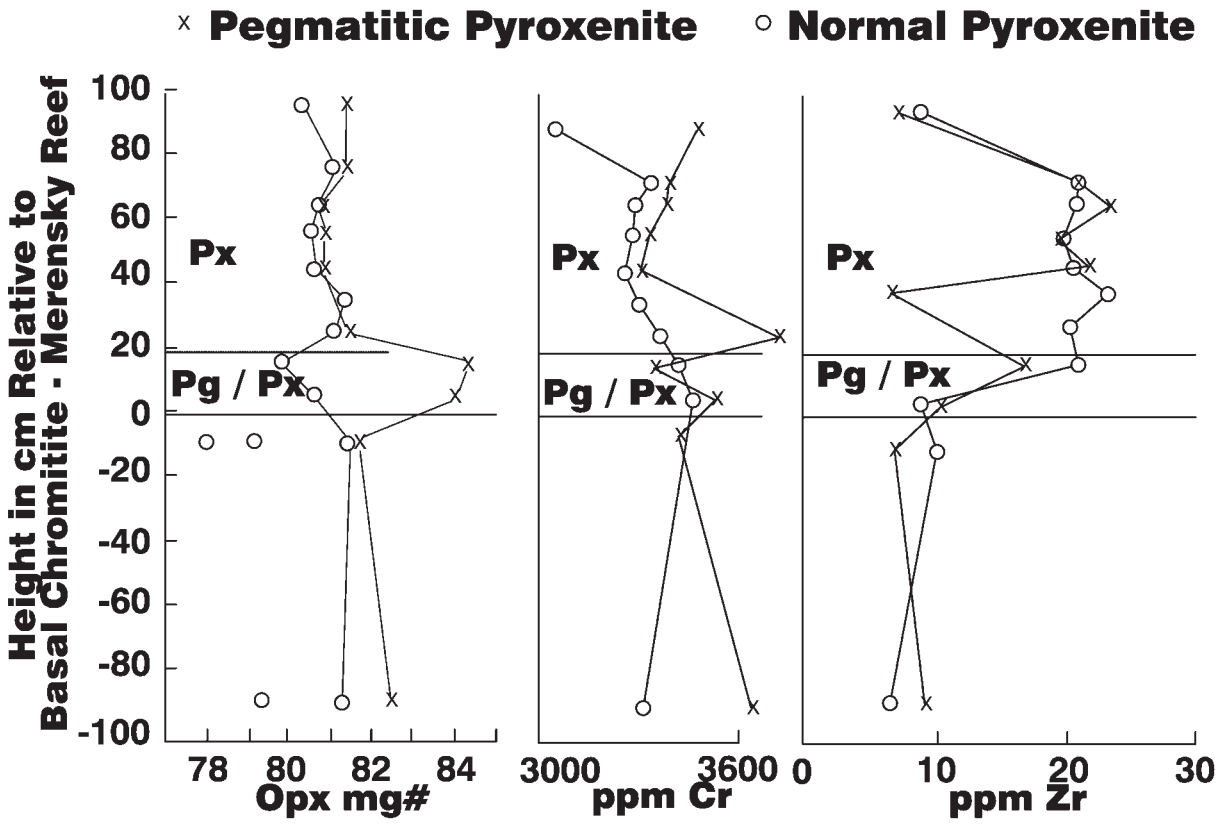

Fig. 6. Mg value, and Cr and Zr content (ppm) in the orthopyroxene mineral concentrates vs height in the underlying rocks and the Merensky pyroxenite. (See Fig. 5 caption for further details.)

orthopyroxene *in situ* and engulfed the chromite grains in their original stratigraphic position. We, therefore, suggest that the unusual textures shown in Figs 3a–c and 4 are the result of post-cumulus textural growth and are not primary igneous textures. The timing of this recrystallization process relative to the accumulation of the crystal pile is discussed below.

FORMATION OF THE PEGMATITIC PYROXENITE

In many hypotheses the genesis of the pegmatitic texture has become inextricably entwined with that of the PGE mineralization, and so there is frequent reference to the mineralization itself in the following discussion. However, as noted above, PGE mineralization occurs in the northern part of Impala Mine where there is no pegmatitic pyroxenite and also occurs in the footwall anorthosite (Cawthorn *et al.*, 2002*b*). In sections of the eastern limb (compare profiles from Lebowa and Winnaarshoek mines in Fig. 2), mineralization occurs in normal pyroxenite, up to 2 m above the pegmatitic pyroxenite zone (Mossom, 1986). Hence, we do not consider the formation of pegmatitic texture and mineralization to be necessarily directly related.

Wagner (1929) described the pegmatitic textures in detail, but offered no suggestions as to their genesis. The next generation of publications after Wagner was based largely on information from the Rustenburg Platinum Mine, the geology of which has strongly influenced views on the nature of the mineralized part of the Merensky Unit and its genesis. Coertze (1958) suggested that the pegmatitic pyroxenite was a younger intrusion, but its occurrence between the underlying anorthosite and overlying pyroxenite, with chromitite on both contacts, is difficult to explain by this model. Hess (1960), Wager & Brown (1968) and Cousins (1969) suggested that the pyroxenite to anorthosite cycles resulted from injection of new magma batches. Only Wager & Brown (1968) offered comment on the genesis of the pegmatitic textures, suggesting that they were crescumulates, but did not elaborate. These three contributions implied that purely magmatic processes were operative for both the pegmatitic textures and the mineralization.

Lauder (1970) suggested a hydrothermal and post-magmatic concentration process for the PGE mineralization, and that this fluid also produced the pegmatitic

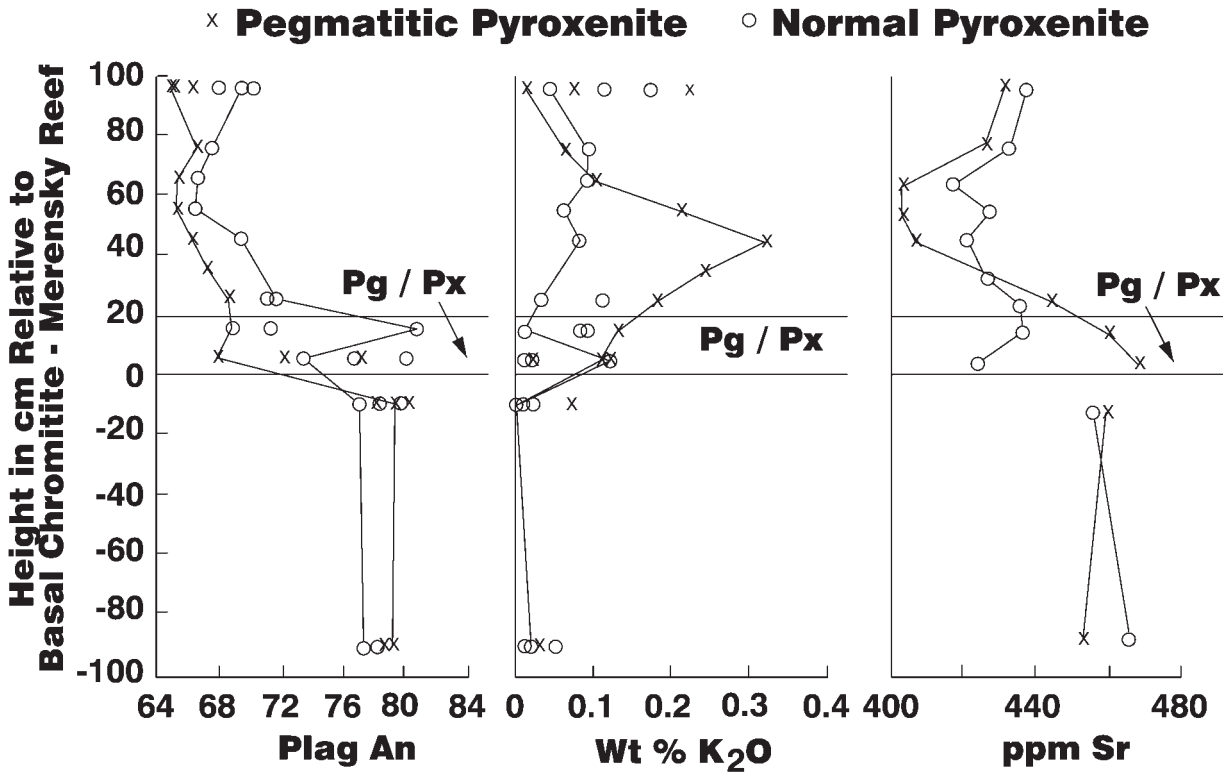

Fig. 7. An content, wt % K_2O and ppm Sr in the plagioclase mineral concentrates vs height in the underlying rocks and the Merensky pyroxenite. (See Fig. 5 caption for further details.)

textures. A number of variations on this theme have evolved, all of which invoke a secondary process of upward migration of a fluid, and its trapping beneath a pre-existing layer of varying rock types. The nature of the upward-mobile fluid varies in these models. Vermaak (1976) concluded that a mat of plagioclase crystals (which would ultimately become the Merensky anorthosite layer) aggregated at some suspended level in the magma chamber. The underlying magma began to crystallize the Merensky pyroxenite. An upward migrating fluid penetrated this layer, but was trapped below this plagioclase mat. Subsequent crystallization of this fluid-enriched magma produced the pegmatitic pyroxenite and the PGE-bearing sulphide mineralization. In this model, the fluid was a residual silicate magma emanating from the underlying succession. Subsequently, the role of a volatile component (dominated by H_2O, CO_2, and Cl), considered to have been derived from the differentiating magma in the footwall, has been examined (Mathez, 1989; Nicholson & Mathez, 1991; Boudreau, 1995, 1999; Boudreau & Meurer, 1999). Possible contributions to this volatile phase from floor rocks were suggested by Ballhaus & Stumpfl (1985), who implied a low-temperature, subsolidus process. In the model of Nicholson & Mathez (1991) this added fluid caused the remelting of part of the original Merensky pyroxenite, implying temperatures above the water-rich solidus.

Kinloch (1982), Ballhaus (1988) and Boudreau (1992, 1999) suggested that the initial volatile escape might have been syn-magmatic, erupting through sites of potholes. This event would have pre-dated the deposition of the pyroxenite, and could not have produced the pegmatitic textures in the pyroxenite. However, these models do not preclude a continuum of degassing to lower temperatures when the pyroxenite was in place, and so could have produced the pegmatitic texture.

A fundamentally different interpretation was presented by Naldrett *et al.* (1986) and developed by Barnes & Campbell (1988). Their arguments were focused on the origin of the mineralization, but pertain to the formation of the pegmatitic textures. They suggested that the Merensky pyroxenite was a layer that had an original higher proportion of interstitial liquid component than adjacent layers, and that the fluid or incompatible-element enriched component was not added subsequently. They suggested that the overlying layer (Merensky anorthosite) was a relatively impermeable adcumulate with minimal interstitial component that trapped the more abundant, incompatible-element enriched component in the underlying Merensky pyroxenite. Because of this proposed greater interstitial liquid

component, this layer was able to texturally re-equilibrate more extensively than layers with less liquid to produce the coarse grain size. In yet another variant of this process, Barnes & Maier (2002*b*) suggested that the primary crystals of pyroxene were forced together by compaction.

An alternative view is that the coarse texture is the result of intraplutonic quenching. In this model, the pegmatitic pyroxenite is considered to have a primary texture that results from a moderate cooling rate, induced by addition of a new magma, which is hotter than the existing magma in the chamber. The specific balance between degree of supercooling, nucleation and diffusion rates resulted in few large crystals developing. Examples of this process were quoted by Morse (1986) and Ballhaus & Glikson (1989), although they did not specifically highlight the Merensky pegmatitic pyroxenite.

We now review these models in the light of the data obtained as part of this study.

Intraplutonic quenching

A number of features are not consistent with this mechanism for the formation of the pegmatitic textures. The textures in Fig. 3 show that considerable recrystallization has taken place to produce the coarse textures, which could not be produced during relatively rapid cooling. Intraplutonic quenching would produce a rock with a higher proportion of trapped liquid than in the adjacent cumulate rocks. The low concentrations of incompatible elements through the studied sections (Fig. 5) suggest that the pegmatitic rocks are not enriched in the liquid component, relative to adjacent, obviously cumulate rocks.

Role of an added fluid

Many of the models summarized above require the addition of a fluid or residual magma to a pre-existing incompletely consolidated, cumulate mush that ultimately became the pegmatitic pyroxenite layer. Such a residual phase should have been enriched in incompatible elements and low-melting temperature components. It would have crystallized incompatible-element enriched minerals (Mathez, 1995), resulting in enriched whole-rock compositions. Whereas the model of Naldrett *et al.* (1986) and Barnes & Campbell (1988) does not require addition of this component, they suggested that there was a greater proportion of interstitial liquid in the original crystal mush than in the overlying layers. Using the terminology of Wager *et al.* (1960) the layer would have had a greater orthocumulate content than other layers. In these models, it is also required that this residual component be trapped (permanently or temporarily) beneath a less permeable layer or that the migrating fluid dissolved into the interstitial liquid, producing a zone in which this interstitial liquid had higher concentrations of residual components. Both processes would have produced a layer that would appear to have more orthocumulate component than all the other layers in the succession, especially the overlying layer. Petrographic determination of the proportion of adcumulus to orthocumulus phases in layered igneous rocks is very subjective, especially in those that have undergone recrystallization. It is not only the pegmatitic layer that shows signs of recrystallization. Hunter (1996) and Boorman *et al.* (2004) showed that many of the pyroxenites and anorthosites of the Bushveld intrusion have undergone textural annealing. As a result, the geochemical method for determining the proportion of orthocumulus component in a rock is applied here.

Wager (1960) pioneered this approach to determining the proportion of trapped liquid, using P_2O_5 contents in rocks from the Skaergaard intrusion below the level of appearance of cumulus apatite. In our study, the P_2O_5 content is close to detection limits because the studied samples are all close to adcumulates. Instead, we use Zr and K_2O as relatively incompatible elements. Orthopyroxene contains 5–20 ppm Zr (Cawthorn, 1996; Wilson *et al.*, 1999; and Tables 2 and 3) and hence the whole-rock Zr content of a pyroxene-rich rock should be higher than that of a plagioclase-dominated rock for the same proportion of interstitial component. Thus, absolute values of Zr cannot be used to determine the trapped liquid content in all rock types. A similar limitation applies to K_2O because the plagioclase in this study contains an average of 0·1% K_2O (Tables 2 and 4). However, if two pyroxenite layers are being compared then the relative concentrations of Zr and K_2O will indicate differences in trapped liquid contents. The data from this study are shown in Figs 5 and 8. In the vertical profiles it can be seen that these elements are not enriched in the pegmatitic rocks relative to overlying normal pyroxenite. In fact, the highest abundances always occur at a height of about 40–60 cm above the basal contact, regardless of grain size of the rock.

The plot of K_2O vs Zr in pyroxenites (Fig. 8) shows an extremely poor linear correlation. Pure orthopyroxene would plot at 5–20 ppm Zr and 0% K_2O, and the residual liquid at this level of the intrusion can be calculated from the experimental data of Cawthorn & Davies (1983) to have contained about 120 ppm Zr and 1·2% K_2O (Li *et al.*, 2001). Ideally, if pyroxenite samples contained only cumulus orthopyroxene and trapped liquid they ought to define a linear trend between cumulate orthopyroxene and liquid compositions. However, the data show a large scatter, typically to the Zr-rich side of the trend. What is important here is that, on average, the pegmatitic rocks tend to have lower, not higher, abundances of these two elements than the normal pyroxenite and are not obviously enriched in residual liquid component.

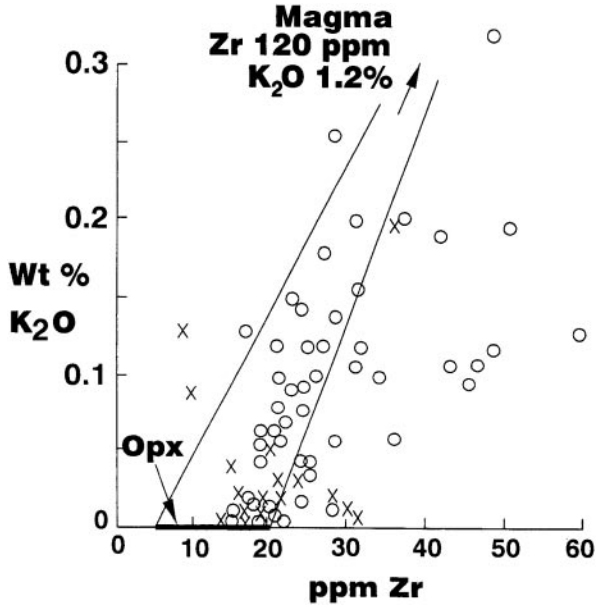

Fig. 8. Variation of K_2O vs Zr for samples from the Merensky pyroxenite. Symbol designation differs slightly from that in Figs 5–7. Only the samples of the pegmatitic pyroxenite are shown by crosses (×), and all the samples of pyroxenite with normal grain size by open circles, whether they come from a profile above the pegmatitic pyroxenite or where there is no pegmatitic pegmatite. It should be noted that the abundances of these two incompatible elements are typically less in the pegmatitic pyroxenite than in the normal pyroxenite. The composition of the inferred magma from which these rocks accumulated plots at 120 ppm Zr and 1·2% K_2O, based on the experimental study of Cawthorn & Davies (1983) and calculations by Li *et al.* (2001). The two lines project towards that composition from the cumulus orthopyroxene that contains 5–20 ppm Zr (Tables 2 and 3).

The above data are not unique. Three other detailed and systematic profiles through the Merensky pegmatitic and normal pyroxenite were presented by Lee (1983), Wilson *et al.* (1999), who only quoted Zr data, and Barnes & Maier (2002*b*). Their data are reproduced in Fig. 9. Where the pegmatitic rocks are less than 40 cm thick [profile of Lee (1983), Fig. 9b, and second profile of Wilson *et al.* (1999), Fig. 9d] the pegmatitic rocks have lower abundances than the overlying pyroxenite. Also, at a height to 40–70 cm above the basal contact there is a peak in abundances, as also recorded in this study. Where the pegmatitic rocks are thicker [profile of Barnes & Maier (2002*b*), Fig. 9a, and first profile of Wilson *et al.* (1999), Fig. 9c] the peak in these elements is again at 40–70 cm above the base, but within the pegmatitic facies. Apart from this peak other values in the pegmatitic pyroxenite are comparable with those in the overlying pyroxenite. In our study, the 20 cm thick pegmatitic pyroxenite contains less than 0·05% K_2O (Fig. 7). The 70 cm thick pegmatitic pyroxenite of Barnes & Maier (2002*b*) also has low values for K_2O at the base, increasing upward to 0·3% at 40 cm height. The 2 m-thick pegmatitic pyroxenite of Wilson *et al.* (1999) (Fig. 9c) has low abundances of Zr at the base increasing upward to 70 cm, and then decreasing toward the top. We infer from all these studies that where the pegmatitic layer is thin it has low abundances of these incompatible trace elements. What is distinctive is that in all profiles, elevated values occur, typically 40 cm or slightly higher, above the base of the pyroxenite, regardless of the rock type (pegmatitic or normal pyroxenite).

In an extension of the data obtained on samples studied by Wilson *et al.* (1999), Arndt *et al.* (2005) noted that much higher concentrations of incompatible elements, such as Th, exist in pyroxenites than in over- and underlying norites. However, inspection of their figs 3 and 6 shows that both pegmatitic and non-pegmatitic pyroxenites are equally enriched. They also discussed the relevance of their data to the debate about the role of a residual fluid, and we concur with many of their observations.

Compaction processes

The possible movement of interstitial magma within the cumulate pile has been considered important in models that involve infiltration metasomatism and compaction. Mathez *et al.* (1997) envisaged a process whereby the interstitial magma in the crystal pile below the level of the Merensky Reef percolated vertically, and was trapped (or perhaps only temporarily retarded) beneath the Merensky anorthosite. They suggested that the relative rates of crystal accumulation vs compaction at this level in the intrusion resulted in the formation of a column of crystal mush up to 350 m thick. Their calculations of compaction rates were based entirely on the viscosity of the crystals and their rates of deformation, as defined by McKenzie (1984, 1987). However, other processes, collectively called crystal ageing (Walker *et al.*, 1985, 1988; Hunter, 1987, 1996; Boudreau, 1994), may also have been occurring together with deformation, increasing the rate at which the porosity in the crystal mush decreased. Near the level of the Merensky Reef, the average rate of accumulation would have been about 7 cm per year (Cawthorn & Walraven, 1998). Walker *et al.* (1988) showed experimentally that small olivine crystals annealed into an almost pure adcumulate (1% interstitial liquid) within weeks. They also showed the formation of an essentially adcumulate texture adjacent to liquid with no crystals. Such observations need to extrapolated with extreme caution, as rates and even mechanisms of growth vary enormously depending upon mineral type (Cabane *et al.*, 2005). Boorman *et al.* (2004) identified a further problem in such processes, by showing that the rate of crystal ageing was dramatically reduced in a bimineralic cumulate because of locking between grains of different minerals (in this case orthopyroxene and plagioclase).

We note a paradox in the compaction model of McKenzie (1987) and Mathez *et al.* (1997), namely the

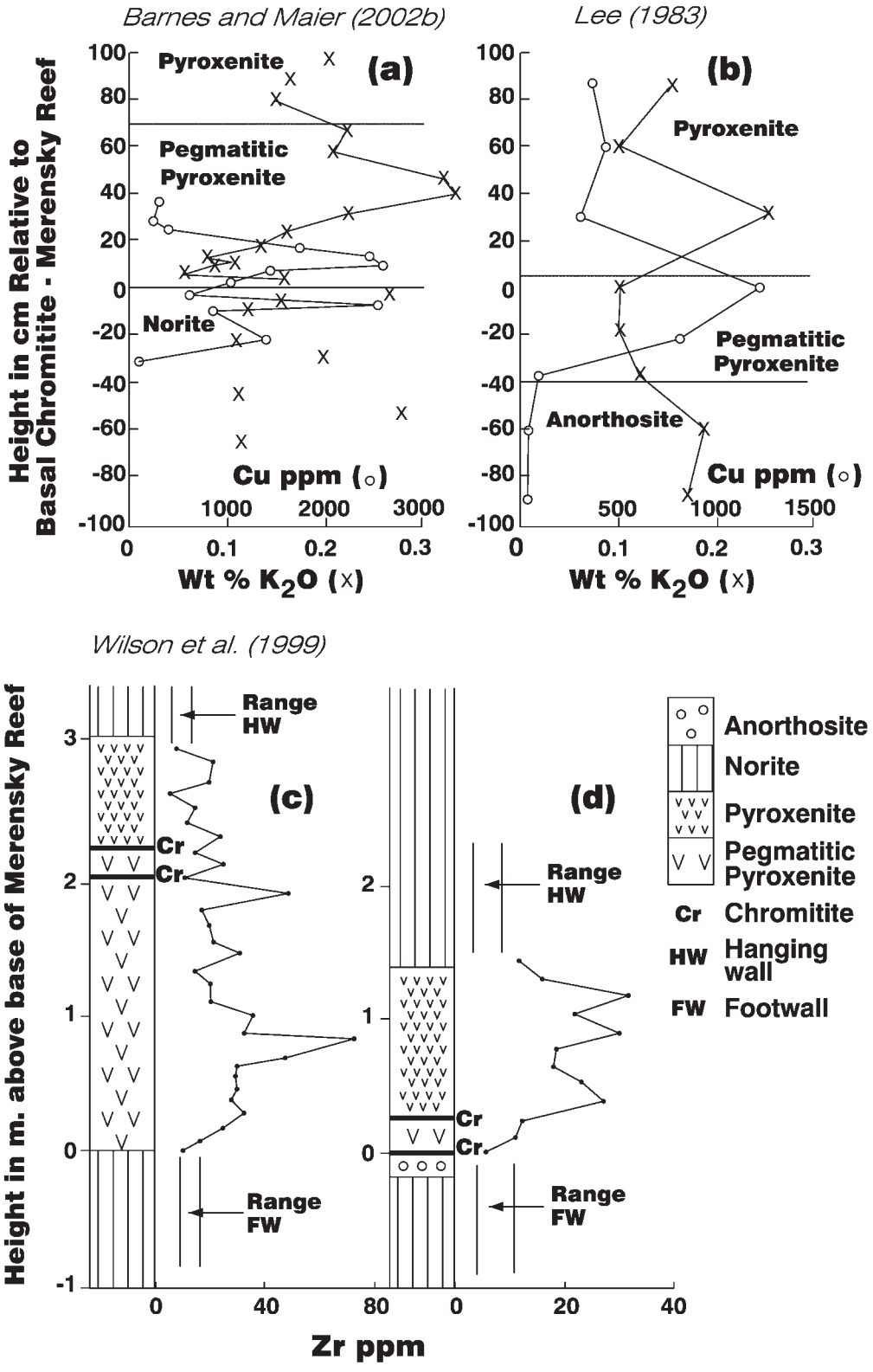

Fig. 9. Trace element abundances in profiles through the Merensky pyroxenite from various sources. (a) and (b) K_2O (×) and Cu (○) vs height from the data of Lee (1983) and Barnes & Maier (2002*b*). (c) and (d) Zr vs height for samples from two sections (one with thick and one with thin pegmatitic pyroxenite) from Wilson *et al.* (1999). In all profiles, most samples of pegmatitic rocks show element concentrations comparable with those in the overlying normal pyroxenite, but high values occur at a height of 40–60 cm above the basal contact, regardless of rock type.

predicted final porosity. McKenzie (1987) argued that porosities of as low as 1% would rapidly be achieved during compaction (with reference to a pure olivine assemblage). Mathez *et al.* (1997, p. 29) similarly concluded that 'a residual porosity of more than a few percent in an accumulating pile of crystals is not plausible for intrusions the size of the Bushveld Complex'. All estimates of residual porosity at the level of the Upper Critical Zone give values of 10–20% (Cawthorn, 1996, 1999; Maier & Barnes, 1998; Meurer & Boudreau, 1998; Boorman *et al.*, 2004), which strongly contrast with the predictions of this compaction model.

In terms of the trapping (permanently or temporarily) or retarding of a rising residual component, Mathez *et al.* (1997) suggested that the Merensky anorthosite acted as a barrier to upward porous flow and caused the remelting and/or recrystallization of a pre-existing pyroxenite into a pegmatitic texture. In the numerous profiles, generalized in Fig. 2, and in the specific profiles in Figs 5–7 and 9, we note that the pegmatitic pyroxenite almost always occurs at the base of the entire Merensky pyroxenite. The pegmatite can be overlain by up to 6 m of pyroxenite of normal grain size in the Impala Mine. If the anorthosite had been the trapping structure, we would expect the pegmatite to have developed at the top of the pyroxenite unit, not the base.

Barnes & Maier (2002*b*) argued for a different effect of compaction that was physical rather than chemical. They noted that the orthopyroxene grains were complex grains that appeared to be made of a number of smaller grains that had been forced together and developed into one large grain. They appealed to a compaction process to achieve this effect. They did not discuss how thick the overlying crystal pile was during compaction, nor what provided this additional force, specific to the Merensky pegmatitic pyroxenite. Also, the mechanism of crystallographic reorientation of multiple small grains was not discussed.

Syn-magmatic processes

We suggest a rather different timing and driving force for the recrystallization process that produced the pegmatitic pyroxenite. The model we present is a development and elaboration of the processes suggested by Cawthorn & Barry (1992), Viljoen (1999) and Viring & Cowell (1999) and termed 'reconstitution' by them. We concur with Hunter (1996) and Boorman *et al.* (2004) that significant textural maturity has occurred as a result of various processes that can be collectively called 'crystal ageing'. However, we suggest that a considerable proportion of this ageing occurred close to the crystal–liquid interface. For layers with a typical grain size, we envisage a process in which primary accumulation of grains occurred (whether by sinking or *in situ* growth is not crucial in this argument). The primary porosity then decreased by crystal ageing to a value of 10–20% while the crystals were still very close to the crystal–liquid interface. Thereafter, this proportion of liquid remained trapped during subsequent cooling to be recorded in the incompatible-element abundances of the whole-rocks as the residual porosity (Morse, 1986). In this model, the vertical extent of crystal mush that exceeds this value of 10–20% liquid, and from which further liquid might be extracted, is short (we suggest, no more than a few metres).

We propose that pegmatitic pyroxenite and normal pyroxenite formed as two temporarily distinct layers, and were not part of a single pyroxenite-forming event that was succeeded by replacement of its lower part by a pegmatitic facies. We suggest that the first layer of pyroxene crystals formed, and was possibly up to twice the thickness of the preserved pegmatitic pyroxenite. There then followed a stasis in crystallization, when no further crystal accumulation took place. Such a suspension of crystallization could have been induced by a number of processes. There may have been addition of magma that was superheated. Alternatively, a reduction in pressure could have caused the magma that produced the first pyroxenite layer to have become superheated. The concept of fluctuations in pressure to produce layering has been reviewed by Naslund & McBirney (1986), and its role in initiating sulphide immiscibility discussed by Cawthorn (2005). With specific reference to processes that might produce pressure fluctuation here, we suggest the following. Mass-balance calculations for the entire Bushveld Complex for several elements led Cawthorn & Walraven (1998) to conclude that significant volumes of magma must have been expelled intermittently from the magma chamber. As the magma chamber filled, it progressively expanded laterally, especially southward. For example, the lower chromitite layers are less extensive laterally than the Merensky Reef, which is again less extensive than the vanadiferous magnetitite layers in the Upper Zone. We therefore suggest that there was not only periodic addition of magma that inflated the chamber, but that there was lateral migration of magma to extend the chamber, or expulsion by injection into the sedimentary rocks forming the sides of the chamber. These processes may have resulted in a decrease in the thickness of the magma column, thus reducing the pressure at the base.

If there was a cessation in accumulation of the crystal pile then more efficient crystal ageing could have operated at the crystal–liquid interface. In this process, larger crystals grew at the expense of smaller grains. This process would have had the following effects. A large number of small grains of orthopyroxene might have annealed into single grains. If plagioclase (and chromite) grains had been trapped between previous pyroxene grains they would have been incorporated within these larger grains

as inclusions, retaining their distinctive shapes. We note that this process has been considered the process by which inclusions of silicate minerals are enclosed within enlarged chromite grains (Hulbert & von Gruenewaldt, 1985). Crystal ageing occurs in all crystal mushes (Boorman *et al.*, 2004), but interaction at the crystal–liquid interface with the supernatant magma, rather than at depth in the crystal pile, should permit prolonged and more effective recrystallization. Increase in grain size as a result of crystal ageing is much slower for plagioclase than for pyroxene (Cabane *et al.*, 2005), and so the plagioclase-rich layer below the Merensky pyroxenite would not show such enlarged grain size.

If there had also been dissolution, a number of consequences might be anticipated. The bulk composition of the plagioclase and orthopyroxene may have become slightly more calcic and magnesian, respectively, than the original grains, as inferred by comparison of mineral compositions in pegmatitic and normal pyroxenite (Figs 6 and 7). Greater degrees of melting could have resulted in the formation of olivine and chromite by incongruent melting of the orthopyroxene. The pegmatitic pyroxenite samples have higher chromite and olivine contents than normal pyroxenite (Tables 1 and 2). In this model, the expelled portion of the rock by partial melting, identified in the mass-balance analysis of Nicholson & Mathez (1991), was incorporated into the directly overlying superheated magma. It did not have to find an escape route through nearly solid, overlying rock, as required by the model of Nicholson & Mathez (1991).

The reconstitution process envisaged here involved both recrystallization and remelting; both occurred concurrently. An analogy may be noted in which packed ice cubes in a glass of water may both melt and combine into a single, solid mass. Complete melting would have resulted in the elimination of the original pyroxenite, and subsequent melting of the underlying anorthositic rocks would have become possible. Campbell (1986) suggested that potholes were generated by the addition of hot magma that remelted the underlying rocks. Our modification to this model is to suggest that in reacting with a pyroxenitic rock, there was recrystallization to produce the pegmatitic textures at the same time as dissolution was taking place.

Ultimately, this reconstitution process would have been terminated by one of several events. The magma may have lost all its superheat and resumed crystallization. New magma might have been added that was not superheated and began to crystallize another cycle. A gradual or sudden increase in pressure, possibly as a result of magma addition or tectonic readjustment of the floor of the magma chamber (Carr *et al.*, 1994), would also have caused renewed crystallization. All of these processes could have resulted in another chromitite layer forming, followed by more pyroxenite. In this way, we suggest that the pyroxenite with normal grain size above the pegmatitic pyroxenite was not there when the pegmatitic recrystallization occurred, but is temporarily a totally separate layer, produced from magma of similar composition to that which formed the pegmatitic pyroxenite.

At the Western Platinum Mine (Fig. 2), 20 km east of Rustenburg, the Merensky pyroxenite increases in thickness (Davey, 1992), locally exceeding 10 m in thickness; however, it is not a homogeneous layer. It has a basal chromitite layer and can have up to three other internal chromitite layers (Fig. 2). Pegmatitic textures may be present, typically near the base and also near the uppermost chromitite layer. We suggest that the reason for this increased thickness and complexity of the entire pyroxenite package is because it consists of three vertically stacked, discrete chromite- and pyroxene-forming events, with non-precipitation intervals, during which pegmatite formation may have occurred on more than one occasion from the instantaneous uppermost pyroxenite (Cawthorn *et al.*, 2002a). More effective remelting of these multiple layers has resulted in their variable and partial elimination in the Rustenburg and Impala mines.

INCOMPATIBLE-ELEMENT ENRICHED ZONE

A thin zone of higher than average whole-rock incompatible-element abundances occurs in all profiles in this and other studies (Figs 5 and 9) at relatively constant height above the basal chromitite, and independent of rock type. A process to explain this phenomenon is suggested. It relates to the sinking of immiscible sulphide liquid and upward displacement of silicate liquid (Cawthorn, 1996; Wilson *et al.*, 1999). Most primary accumulation models for the presence of an immiscible sulphide liquid in pyroxenite suggest that the immiscible sulphide and pyroxenes with which it is now associated were coincident. However, Cawthorn (1996) and Cawthorn *et al.* (2002*a*) argued that the sulphide liquid post-dated the formation of the pyroxenite mush, and that, because of its density, percolated down from an overlying layer over a distance of the order of 1 m. In cases of thin pyroxenite layers it even penetrated into the footwall anorthosite. In our model, the immiscible sulphide liquid was coincident with the second, upper pyroxenite, not the first, lower pyroxenite that was converted to the pegmatitic texture. In such a process the sulphide presumably displaced the interstitial silicate liquid that was in the lower (pegmatitic) pyroxenite mush. As a result, the interstitial silicate liquid component in the pegmatitic layer decreased, and the immediately overlying zone may have become enriched. A comparison of the Zr and Cu contents, in Fig. 5, shows that the zone of

relative incompatible-element enrichment (0·2–0·4 m thick) immediately overlies the zone of highest sulphide mineralization, identified by the high Cu contents. Exactly the same relationship is seen in Fig. 9, in the data of Lee (1983) and Barnes & Maier (2002*b*). This exchange of sulphide and silicate liquid would have been driven by density contrast between the two liquids without any significant change in the silicate mineral framework.

CUMULUS AND INTERCUMULUS PLAGIOCLASE IN THE MERENSKY PYROXENITE

Vermaak (1976) referred to the Merensky pyroxenite as containing cumulus orthopyroxene and intercumulus plagioclase. This statement has been frequently repeated, with suggestions that the typical proportions were 70% cumulus pyroxene and 30% intercumulus plagioclase. Using the terminology and model of Wager *et al.* (1960), such a statement cannot be rigorously correct. The intercumulus component is presumed to have formed from a trapped magma, but trapped magma cannot form only one mineral. A typical tholeiitic magma would crystallize about 60% plagioclase and 40% of other minerals, mainly pyroxenes. Hence, if there is 30% intercumulus plagioclase in the Merensky pyroxenite there ought to be a further 20% of other intercumulus phases, mainly pyroxene, and the total trapped liquid content would then have to be 50%. It could, perhaps, be argued that the Merensky pyroxenite should therefore be described as having 50% cumulus pyroxene, and 20 and 30% of intercumulus pyroxene and plagioclase, respectively. However, the abundances of incompatible trace elements (K and Zr, and P and Y not included here because of their very low abundances) suggest smaller proportions of trapped liquid, in the range 10–20% (Cawthorn, 1996; Maier & Barnes, 1998; Boorman *et al.*, 2004). Hunter (1996) and Boorman *et al.* (2004) identified significant textural changes in Bushveld pyroxenites and here we describe atypical textures in the pegmatitic pyroxenite. Hence, the use of purely textural criteria to identify cumulus and intercumulus status, and the proportion of adcumulus to orthocumulus overgrowth, is questionable. We also note that the bulk composition of the texturally interstitial plagioclase in the pegmatitic pyroxenite is An_{77} and so is close to a plausible cumulus composition, not that of plagioclase forming from interstitial trapped liquid. We re-examine the status of the plagioclase in these rocks by reference to Fig. 10, in which we present whole-rock data for Al_2O_3 and Zr for the pegmatitic pyroxenite and normal pyroxenite. We suggest that the likely composition of the magma was about 15% Al_2O_3 and 120 ppm Zr, based on the proposed parental magma and extent of fractionation at this level (Cawthorn & Davies, 1983; Cawthorn, 1996; Li *et al.*, 2001). If these pyroxenites were mixtures of cumulus pyroxene and trapped magma only, all compositions should lie on a linear trend between these two compositions. In fact, many of the compositions contain higher Al_2O_3 contents than predicted by such a relationship. Compositions that contain both cumulus pyroxene and plagioclase, and interstitial liquid will fall within the triangle indicated in Fig. 10. We therefore conclude that many of both the pegmatitic and normal pyroxenites contain some cumulus plagioclase, as well as an intercumulus component that would ultimately crystallize as plagioclase, pyroxene and other minor minerals. If there was about 10% trapped liquid, as indicated by the data in Fig. 10a and b, which solidified to a simplified assemblage of 60% plagioclase, and 20% each of orthopyroxene and clinopyroxene, then we would have to designate a typical rock in Fig. 10 as being composed of about 20 and 70% of cumulus plagioclase and orthopyroxene, and 6, 2 and 2% of intercumulus plagioclase, orthopyroxene and clinopyroxene, respectively. That is a much more complicated statement than the first definition at the beginning of this section, but it is a more genetically correct expression of the origin of the total mineralogy. We note that the same chemical relationships apply to the normal pyroxenites (Fig. 10b) as well as to the pegmatitic pyroxenite (Fig. 10a), and so the presence of a cryptic cumulus plagioclase proportion is not a function purely of the atypical pegmatitic texture, but common to normal pyroxenites as well.

It could be argued that the estimate for the trapped liquid composition in Fig. 10 is inappropriate. However, to make all the plagioclase intercumulus would require a liquid that is unrealistically low in Zr or high in Al_2O_3, or both, which we consider unlikely. Further, we suggest that the composition of the plagioclase concentrates from all the pyroxenite samples supports our interpretation that some of it is cumulus. The anorthosites of the Merensky Unit contain abundant cumulus plagioclase with an An content of 78–80 (Vermaak, 1976; Kruger & Marsh, 1985; Naldrett *et al.*, 1986). Based on the topology of the simplified anorthite–albite phase diagram such a composition would have formed from a liquid containing the An and Ab components in the approximate proportion 50–50. If all the plagioclase in the rock formed from this trapped magma its average composition, as approximated by these analyses in Table 4, ought to be close to this value of 50% An. In fact, the average plagioclase composition in the pyroxenites is close to the cumulus composition in the overlying anorthosite, although it is much more variable (Fig. 7). Relative proportions of cumulus and intercumulus phase cannot be quantified; however, the bulk plagioclase compositions suggest that the pegmatitic pyroxenite contains a

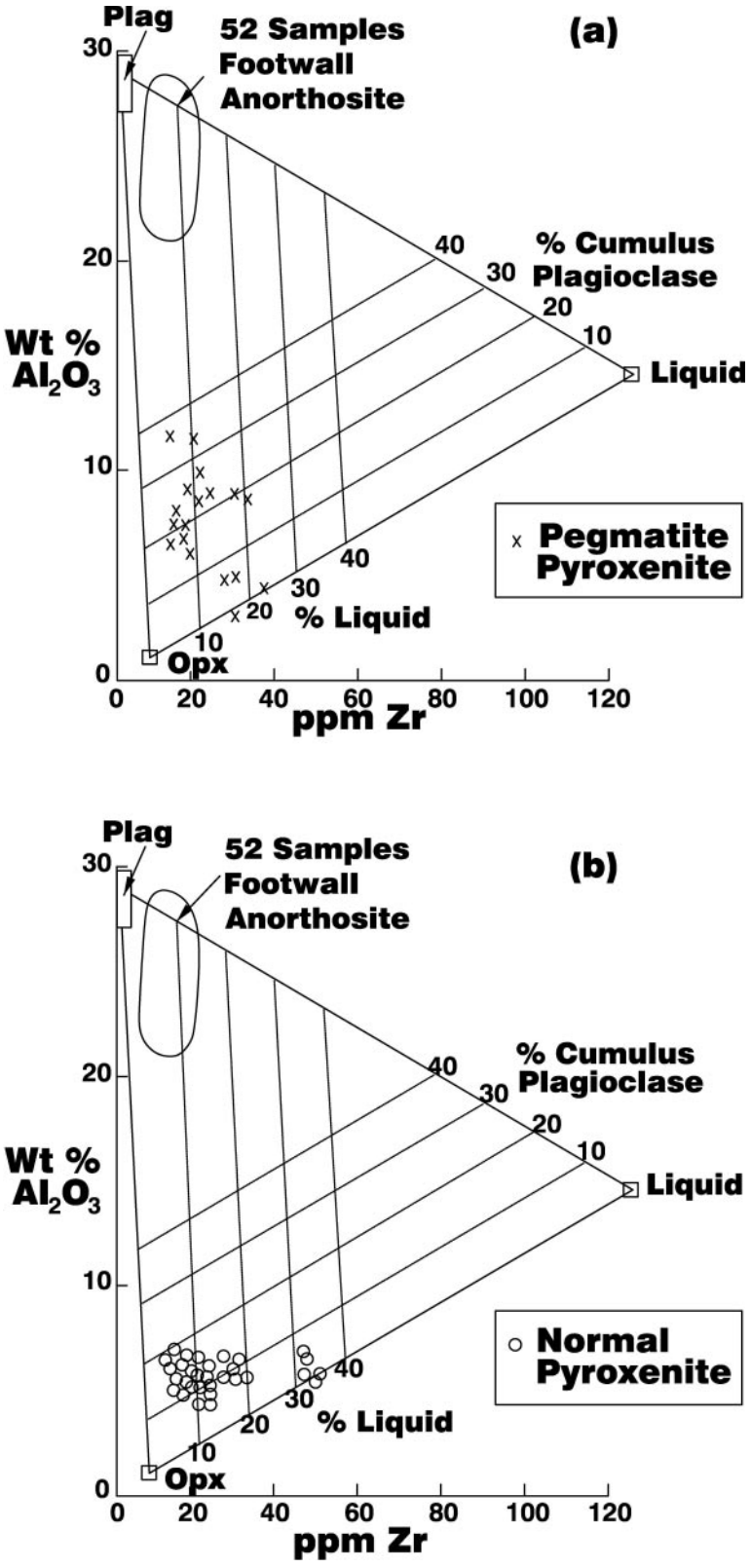

Fig. 10. Al_2O_3 vs Zr for samples from the Merensky pyroxenite. (a) Samples of pegmatitic pyroxenite; (b) samples of normal pyroxenite. Also shown are the average compositions of the cumulus plagioclase and orthopyroxene, and the inferred liquid composition (see text and Fig. 8) at this level in the intrusion. The triangle defined by these three points is graduated to show the relative proportions of cumulus plagioclase and interstitial liquid for these samples.

significant cumulus plagioclase component. The combined texture and mineral compositions suggest that the term heteradcumulate, as defined by Wager *et al.* (1960), might apply.

SUMMARY

We report a number of observations and interpretations about the Merensky Unit at the Impala Platinum Mine, and its mineralization in relation to the host-rocks, and their genesis. The base of the Merensky Unit may be represented by a pegmatitic pyroxenite overlain by a pyroxenite or just a pyroxenite of normal grain size. In the northern part of the mine, the pegmatitic pyroxenite may be totally absent, without affecting PGE grade. The presence of tricuspidate or interstitial-textured plagioclase inside large pyroxene grains in the pegmatitic pyroxenite shows that the coarse grain size is not a primary texture, but has formed by replacement of a previous finer-grained pyroxenite. There is no geochemical evidence for the addition or presence of greater concentrations of fluid or incompatible elements in the pegmatitic facies compared with overlying pyroxenite. Whole-rock analyses show that there was about 10% interstitial magma trapped in these rocks. We suggest that the pegmatitic pyroxenite formed when there was addition of superheated magma or release of pressure in the magma chamber that caused the supernatant magma above the pyroxene crystal mush to become superheated. During the consequent stasis in crystallization, crystal ageing occurred at the interface, producing the pegmatitic texture. Some dissolution also occurred. Once the pegmatitic pyroxenite had formed, there was resumption of crystallization and the overlying normal grain size pyroxenite, with a basal chromitite, was formed. An immiscible sulphide liquid also precipitated with this second pyroxenite-forming event, and percolated approximately 1 m of underlying crystal mush. It displaced some interstitial silicate liquid that ponded above the sulphide-enriched zone, producing high concentration of incompatible elements.

We also suggest that the Merensky pyroxenites are heteradcumulates, as they contain texturally interstitial plagioclase grains that have bulk compositions close to that observed in adjacent layers rich in cumulus plagioclase.

ACKNOWLEDGEMENTS

We are very grateful to Implats, Angloplatinum and Lonplats mining companies and the National Research Foundation for financial support for this project, and Implats for great assistance with borehole logs, samples, discussion and permission to publish. We thank Tony Naldrett, Alan Boudreau and Nick Arndt for their comments on this manuscript. Also thanks go to Sharon Turner, Lyn Whitfield and Di du Toit for XRF and drafting assistance.

REFERENCES

Arndt, N. T., Jenner, J., Ohnenstetter, M., Deloule, E. & Wilson, A. H. (2005). Trace elements in the Merensky Reef and adjacent norites, Bushveld Complex, South Africa. *Mineralium Deposita* **40**, 550–575.

Ballhaus, C. (1988). Potholes of the Merensky Reef at Brakspruit Shaft, Rustenburg Platinum Mines: primary disturbances in the magmatic stratigraphy. *Economic Geology* **83**, 1140–1158.

Ballhaus, C. & Glikson, A. Y. (1989). Magma mixing and intraplutonic quenching in the Wingellina Hills Intrusion, Giles Complex, Central Australia. *Journal of Petrology* **30**, 1443–1469.

Ballhaus, C. & Stumpfl, E. F. (1985). Occurrence and petrological significance of graphite in the Upper Critical Zone, western Bushveld Complex, South Africa. *Earth and Planetary Science Letters* **74**, 58–68.

Barnes, S. J. & Campbell, I. H. (1988). Role of late magmatic fluids in Merensky-type platinum deposits: a discussion. *Geology* **16**, 488–491.

Barnes, S.-J. & Maier, W. D. (2002*a*). Platinum-group element distribution in the Rustenburg Layered Suite of the Bushveld Complex, South Africa. In: Cabri, L. J. (ed.) *The Geology, Geochemistry, Mineralogy and Beneficiation of Platinum-Group Elements. Canadian Institute of Mining, Metallurgy and Petroleum, Special Volume* **54**, 431–458.

Barnes, S.-J. & Maier, W. D. (2002*b*). Platinum-group elements and microstructures from Impala Platinum Mines, Bushveld Complex. *Journal of Petrology* **43**, 171–198.

Boerst, K. D. (2001). Geochemistry of the Merensky Reef at Impala Platinum Mine, western Bushveld Complex. M.Sc thesis, University of the Witwatersrand, 81 pp.

Boorman, S., Boudreau, A. E. & Kruger, F. J. (2004). The Lower Zone–Critical Zone transition of the Bushveld Complex: a quantitative textural study. *Journal of Petrology* **45**, 1209–1235.

Boudreau, A. E. (1992). Volatile overpressure in layered intrusions and the formations of potholes. *Australian Journal of Earth Sciences* **39**, 277–287.

Boudreau, A. E. (1994). Crystal aging in two crystal, two component systems and the formation of fine-scale layering. *South African Journal of Geology* **97**, 473–485.

Boudreau, A. E. (1995). Some geochemical considerations for platinum-group-element exploration in layered intrusions. *Exploration and Mining Geology* **4**, 215–225.

Boudreau, A. E. (1999). Fluid fluxing of cumulates: the J-M Reef and associated rocks of the Stillwater Complex, Montana. *Journal of Petrology* **40**, 755–772.

Boudreau, A. E. (2004). PALLADIUM, a program to model the chromatographic separation of the platinum-group elements, base metal and sulfur in a solidifying pile of igneous crystals. *Canadian Mineralogist* **42**, 393–404.

Boudreau, A. E. & Meurer, W. P. (1999). Chromatographic separation of the platinum-group elements, gold, base metals and sulfur during degassing of a compacting and solidifying igneous crystal pile. *Contributions to Mineralogy and Petrology* **134**, 174–185.

Boudreau, A. E., Mathez, E. A. & McCallum, I. S. (1986). Halogen geochemistry of the Stillwater and Bushveld Complexes: evidence for transport of the platinum-group elements by Cl-rich fluids. *Journal of Petrology* **27**, 967–986.

Cabane, H., Laporte, D. & Provost, A. (2005). An experimental study of Ostwald ripening of olivine and plagioclase in silicate melts: implications for the growth and size of crystals in magmas. *Contributions to Mineralogy and Petrology* **150**, 37–53.

Campbell, I. H. (1986). A fluid dynamic model for the potholes of the Merensky Reef. *Economic Geology* **81**, 1118–1125.

Carr, H. W., Groves, D. I. & Cawthorn, R. G. (1994). The importance of syn-magmatic deformation in the formation of Merensky Reef potholes in the Bushveld Complex. *Economic Geology* **89**, 1398–1410.

Cawthorn, R. G. (1996). Re-evaluation of magma compositions and processes in the uppermost Critical Zone of the Bushveld Complex. *Mineralogical Magazine* **60**, 131–148.

Cawthorn, R. G. (1999). Permeability of footwall cumulates to the Merensky Reef, Bushveld Complex. *South African Journal of Geology* **102**, 293–302.

Cawthorn, R. G. (2005). Pressure fluctuations and the formation of the PGE-rich Merensky and chromitite reefs, Bushveld Complex. *Mineralium Deposita* **40**, 231–235.

Cawthorn, R. G. & Barry, S. D. (1992). The role of intercumulus residua in the formation of pegmatoid associated with the UG2 chromitite, Bushveld Complex. *Australian Journal of Earth Sciences* **39**, 263–276.

Cawthorn, R. G. & Davies, G. (1983). Experimental data at 3 kbars pressure on parental magma to the Bushveld Complex. *Contributions to Mineralogy and Petrology* **83**, 128–135.

Cawthorn, R. G. & Walraven, F. (1998). Emplacement of crystallization time for the Bushveld Complex. *Journal of Petrology* **39**, 1669–1687.

Cawthorn, R. G., Merkle, R. K. W. & Viljoen, M. J. (2002*a*). Platinum-group element deposits in the Bushveld Complex, South Africa. In: Cabri, L. J. (ed.) *The Geology, Geochemistry, Mineralogy and Beneficiation of Platinum-Group Elements. Canadian Institute of Mining, Metallurgy and Petroleum, Special Volume* **54**, 389–430.

Cawthorn, R. G., Lee, C. A., Schouwstra, R. & Mellowship, P. (2002*b*). Relations between PGE and PGM in the Bushveld Complex. *Canadian Mineralogist* **40**, 311–328.

Cawthorn, R. G., Barnes, S. J., Ballhaus, C. & Malitch, K. N. (2005). Platinum-group element, chromium and vanadium deposits in mafic and ultramafic rocks. *Economic Geology, 100th Anniversary volume* 215–249.

Coertze, F. J. (1958). Intrusive relations and ore-deposits in the western part of the Bushveld Igneous Complex. *Transactions of the Geological Society of South Africa* **61**, 387–392.

Cousins, C. A. (1969). The Merensky Reef of the Bushveld Igneous Complex. *Economic Geology Monograph* **4**, 239–251.

Davey, S. R. (1992). Lateral variations within the upper Critical Zone of the Bushveld Complex on the farm Rooikoppies 297 JQ, Marikana, South Africa. *South African Journal of Geology* **95**, 141–149.

Eales, H. V. (1987). Upper Critical Zone chromitite layers at R.P.M. Union Section Mine, western Bushveld Complex. In: Stowe, C. W. (ed.) *Evolution of Chromium Ore Fields*. New York: Van Nostrand and Reinhold, pp. 109–143.

Eales, H. V. & Cawthorn, R. G. (1996). The Bushveld Complex. In: Cawthorn, R. G. (ed.) *Layered Intrusions*. Amsterdam: Elsevier, pp. 181–225.

Eales, H. V., Maier, W. D. & Teigler, B. (1991). Corroded feldspar inclusions in orthopyroxene and olivine of the Lower and Critical Zones, Western Bushveld Complex. *Mineralogical Magazine* **55**, 479–486.

Eales, H. V., Teigler, B. & Maier, W. D. (1993). Cryptic variations of minor elements Al, Cr, Ti and Mn in Lower and Critical Zone orthopyroxenes of the western Bushveld Complex. *Mineralogical Magazine* **57**, 257–264.

Hatton, C. J. & von Gruenewaldt, G. (1987). The geological setting and petrogenesis of the Bushveld chromitite layers. In: Stowe, C. W. (ed.) *Evolution of Chromium Ore Fields*. New York: Van Nostrand and Reinhold, pp. 109–143.

Hess, H. H. (1960). *Stillwater Igneous Complex, Montana: a Quantitative Mineralogical Study*. *Geological Society of America, Memoirs* **80**, 230 pp.

Hulbert, L. J. & von Gruenewaldt, G. (1985). Textural and compositional features of chromite in the Lower and Critical Zones of the Bushveld Complex south of Potgietersrus. *Economic Geology* **80**, 872–895.

Hunter, R. H. (1987). Textural equilibrium in layered igneous rocks. In: Parsons, I. (ed.) *Origins of Igneous Layering*. Dordrecht: Reidel, pp. 473–503.

Hunter, R. H. (1996). Texture development in cumulate rocks. In: Cawthorn, R. G. (ed.) *Layered Intrusions*. Amsterdam: Elsevier, pp. 77–102.

Kinloch, E. D. (1982). Regional trends in the platinum-group mineralogy of the Critical Zone of the Bushveld Complex. *Economic Geology* **77**, 1328–1347.

Kruger, F. J. & Marsh, J. S. (1985). The mineralogy, petrology and origin of the Merensky Cyclic Unit in the western Bushveld Complex. *Economic Geology* **80**, 958–974.

Lauder, W. R. (1970). Origin of the Merensky Reef. *Nature* **227**, 365–366.

Lee, C. A. (1983). Trace and platinum-group element geochemistry and the development of the Merensky Reef of the Bushveld Complex. *Mineralium Deposita* **18**, 173–180.

Lee, C. A. (1996). A review of mineralization in the Bushveld Complex and some other layered mafic intrusions. In: Cawthorn, R. G. (ed.) *Layered Intrusions*. Amsterdam: Elsevier, pp. 103–146.

Leeb-du Toit, A. (1986). Impala Platinum Mines. In: Anhaeusser, C. R. & Maske, S. (eds) *Mineral Deposits of Southern Africa*, II. Geological Society of South Africa, Special Publication **2**, 1091–1006.

Li, C., Maier, W. D. & de Waal, S. A. (2001). The role of magmatic mixing in the genesis of PGE mineralization in the Bushveld Complex: thermodynamic calculations and new interpretations. *Economic Geology* **96**, 653–662.

Maier, W. D. & Barnes, S.-J. (1998). Concentrations of rare earth elements in silicate rocks of the Lower, Critical and Main Zones of the Bushveld Complex. *Chemical Geology* **150**, 85–103.

Mathez, E. A. (1989). The role of vapor associated with mafic magma and controls on its composition. In: Whitney, J. A. & Naldrett, A. J. (eds) *Ore Deposition Associated with Magmas. Reviews in Economic Geology* **4**, 21–31.

Mathez, E. A. (1995). Magmatic metasomatism and formation of the Merensky Reef, Bushveld Complex. *Contributions to Mineralogy and Petrology* **119**, 277–286.

Mathez, E. A., Hunter, R. H. & Kinzler, R. (1997). Petrologic evolution of partially molten cumulate: the Atok section of the Bushveld Complex. *Contributions to Mineralogy and Petrology* **129**, 20–34.

McKenzie, D. (1984). The generation and compaction of partially molten rocks. *Journal of Petrology* **25**, 713–765.

McKenzie, D. (1987). The compaction of igneous and sedimentary rocks. *Journal of the Geological Society, London* **144**, 299–307.

Meurer, W. P. & Boudreau, A. E. (1998). Compaction of igneous cumulates, part I: Geochemical consequences for cumulates and liquid fractionation trends. *Journal of Geology* **106**, 281–292.

Morse, S. A. (1984). Cation diffusion in plagioclase feldspar. *Science* **225**, 504–505.

Morse, S. A. (1986). Convection in aid of adcumulus growth. *Journal of Petrology* **27**, 1183–1214.

Mossom, R. J. (1986). The Atok Platinum Mine. In: Anhaeusser, C. R. & Maske, S. (eds) *Mineral Deposits of Southern Africa*, II. Geological Society of South Africa, Special Publication **2**, 1143–1154.

Naldrett, A. J., Gasparrini, E. C., Barnes, S. J., von Gruenewaldt, G. & Sharpe, M. R. (1986). The Upper Critical Zone of the Bushveld

Complex and the origin of Merensky-type ores. *Economic Geology* **81**, 1105–1117.

Naslund, H. R. & McBirney, A. R. (1996). Mechanisms of formation of igneous layering. In: Cawthorn, R. G. (ed.) *Layered Intrusions*. Amsterdam: Elsevier, pp. 1–44.

Nicholson, D. M. & Mathez, E. A. (1991). Petrogenesis of the Merensky Reef in the Rustenburg section of the Bushveld Complex. *Contributions to Mineralogy and Petrology* **107**, 293–309.

Schurmann, L. W. (1993). *The geochemistry and petrology of the Upper Critical Zone of the Boshoek section of the western Bushveld Complex*. *Bulletin of the Geological Survey of South Africa* **113**, 99 pp.

Tredoux, M., Lindsay, N. M., Davies, G. & McDonald, I. (1995). The fractionation of platinum-group elements in magmatic systems with a suggestion of a novel causal mechanism. *South African Journal of Geology* **98**, 157–167.

Vermaak, C. F. (1976). The Merensky Reef—thoughts on its environment and genesis. *Economic Geology* **71**, 1270–1298.

Viljoen, M. J. (1999). The nature and origin of the Merensky Reef of the western Bushveld Complex based on geological facies and geophysical data. *South African Journal of Geology* **102**, 221–239.

Viring, R. G. & Cowell, M. W. (1999). The Merensky Reef on Northam Platinum Limited. *South African Journal of Geology* **102**, 192–208.

Von Gruenewaldt, G. (1979). A review of some recent concepts of the Bushveld Complex with particular reference to the sulfide mineralization. *Canadian Mineralogist* **17**, 233–256.

Wager, L. R. (1960). The major element variation of the layered series of the Skaergaard intrusion and a re-estimation of the average composition of the hidden layered series and the successive residual magmas. *Journal of Petrology* **1**, 364–398.

Wager, L. R. & Brown, G. M. (1968). *Layered Igneous Rocks*. Edinburgh: Oliver & Boyd, 588 pp.

Wager, L. R., Brown, G. M. & Wadsworth, W. J. (1960). Types of igneous cumulates. *Journal of Petrology* **1**, 73–85.

Wagner, P. A. (1929). *The Platinum Deposits and Mines of South Africa*. Edinburgh: Oliver & Boyd, 326 pp.

Walker, D., Jurewicz, S. & Watson, E. B. (1985). Experimental observation of an isothermal transition from orthocumulus to adcumulus texture. *EOS Transactions, American Geophysical Union* **66**, 362.

Walker, D., Jurewicz, S. & Watson, E. B. (1988). Adcumulus dunite growth in a laboratory thermal gradient. *Contributions to Mineralogy and Petrology* **99**, 306–319.

Willemse, J. (1969*a*). The geology of the Bushveld Igneous Complex, the largest repository of magmatic ore deposits in the world. *Economic Geology Monograph* **4**, 1–22.

Willemse, J. (1969*b*). The vanadiferous magnetic iron ore of the Bushveld Igneous Complex. *Economic Geology Monograph* **4**, 187–208.

Wilson, A. H., Lee, C. A. & Brown, R. T. (1999). Geochemistry of the Merensky Reef, Rustenburg section, Bushveld Complex: controls on the silicate framework and distribution of trace elements. *Mineralium Deposita* **34**, 657–672.